Electronic Supplementary Information for

A selenium-coordinated palladium(II) *trans*-dichloride molecular rotor as a catalyst for site-selective annulation of 2-arylimidazo[1,2-*a*]pyridines

Neha Meena,[a] Shobha Sharma,[b] Ramprasad Bhatt,[a] Vikki N. Shinde,[a] Anurag Prakash Sunda,[c] Nattamai Bhuvanesh,[d] Anil Kumar *[a] and Hemant Joshi *[e]

[a]*Department of Chemistry, Birla Institute of Technology and Science, Pilani Campus, Pilani 333031, India. E-mail: anilkumar@pilani.bits-pilani.ac.in*
[b]*Department of Chemistry, Indian Institute of Technology Delhi, New Delhi 110016, India*
[c]*Department of Chemistry, J. C. Bose University of Science and Technology, YMCA, Faridabad-121006, India*
[d]*Department of Chemistry, Texas A&M University, PO Box 30012, College Station, Texas 77842-3012, USA*
[e]*ISC Laboratory, Department of Chemistry, School of Chemical Sciences and Pharmacy, Central University of Rajasthan, NH-8, Bandarsindri, Ajmer, Rajasthan 305817, India.*
E-mail: hemant.joshi@curaj.ac.in

EXPERIMENTAL SECTION

General. The ligand and complex were synthesized using standard Schlenk techniques. The catalysis reactions were carried out in pressure tube under open air conditions. HPLC grade DMF, CH_2Cl_2, EtOH, EtOAc, hexane, CH_3CN, DMAc, DMSO and xylene were used directly as received. Salicylaldehyde (Sigma Aldrich), benzyl bromide (Spectrochem), K_2CO_3 (Spectrochem), selenium powder (Sigma Aldrich), $NaBH_4$ (Spectrochem), Na_2SO_4 (Spectrochem), $CDCl_3$ (Sigma Aldrich), and $PdCl_2$ (Alfa Aesar, 99.9%) were used as purchased. All other reagents for catalysis reaction were purchased from local commercial sources and used as it is. NMR spectrum were recorded on a Bruker NMRs 400 MHz instruments at ambient probe temperatures and referenced as follows (δ, ppm): ^{1}H, residual internal $CHCl_3$ (7.26); ^{13}C{^{1}H}, internal $CDCl_3$ (77.00). IR spectrums of new ligand and complex were taken on a Nicolet Protége 460 FT-IR spectrometer on KBr pellets. Melting points of new complexes were recorded in an open capillary. HRMS measurements were carried out by electrospray ionization (ESI) method on an Agilent Q-TOF LCMS spectrometer.

Synthesis of bis(2-(benzyloxy)benzyl)selane (2). A three necked round bottom flask was charged with selenium powder (4.00 mmol, 0.316 g) in 40 mL ethanol, and fitted with condenser under N_2 atmosphere. The mixture was refluxed and solid $NaBH_4$ (0.310 g, 8.2 mmol) was added in small portions until the mixture turned into colorless solution. A solution of 1-(benzyloxy)-2-(chloromethyl)benzene (**1**, 0.465 g, 2.00 mmol) in C_2H_5OH (5 mL) was added drop wise with stirring. After 12 h mixture was cooled to room temperature, solvent was reduced (~2 mL) by using rotary evaporated. The residue was placed at the top of a silica column (3 × 14 cm), which was eluted with hexanes (150 mL) and then hexanes/EtOAc (90:10 v/v). The solvent was evaporated from the product containing fractions (assayed by TLC) by rotary evaporation to give **2** as a yellow oil (0.768 g, 1.622 mmol, 81%). Anal. Calcd for $C_{28}H_{26}O_2Se$ (473.47): C, 71.03; H, 5.54. Found: C, 70.92; H, 5.47.

NMR ($CDCl_3$, δ/ppm): **^{1}H** (400 MHz) 7.47-7.45 (m, 2H), 7.38-7.31 (m, 3H), 7.19-7.15 (m, 2H), 6.91-6.83 (m, 2H), 5.01 (s, 2H, OCH_2), 3.87 (s, 2H, SeCH_2); **^{13}C{^{1}H}** (100 MHz) 156.2 (s),

137.2 (s), 130.2 (s), 128.9 (s), 128.5 (s), 127.8 (s), 127.7 (s), 127.2 (s), 120.6 (s), 111.9 (s), 69.9 (s, O*C*H_2), 22.3 (s, Se*C*H_2). **IR** (cm^{-1}, powder film): 3216 (w), 3050 (w), 2875 (w), 1597 (s), 1489 (s), 1450 (s), 1242 (s), 694 (s). HRMS (ESI) calcd for $C_{28}H_{27}O_2Se$ $[M + H]^+$: 475.1176, found 475.1129.

Palladium complex of bis(2-(benzyloxy)benzyl)selane (3). A round bottom flask was charged with **2** (0.473 g, 1.00 mmol), $PdCl_2(CH_3CN)_2$ (0.130 g, 0.50 mmol), acetonitrile (15 mL), and fitted with a condenser. The mixture was stirred (2h) while refluxing. The mixture was then cooled, passed through a short pad of silica gel (18 cm) and washed with CH_3CN (25 mL). The solvent was removed by rotary evaporation and residue was washed with cold *n*-pentane to give **3** as a yellow solid (0.417 g, 0.371 mmol, 74%). m.p: 296-298 ˚C. Anal. Calcd for $C_{56}H_{52}Cl_2O_4PdSe_2$ (1124.25): C, 59.83; H, 4.66. Found: C, 59.91; H, 4.58.

NMR ($CDCl_3$, δ/ppm): **^{1}H** (400 MHz) 7.44-7.39 (m, 3H), 7.36-7.28 (m, 3H), 7.24-7.18 (m, 1H), 6.86-6.81 (m, 2H), 5.00 (s, 2H, OCH_2), 4.56 (d, 2H, J = 11.2 Hz, SeCH_2), 4.14 (d, 2H, J = 11.2 Hz, SeCH_2); **^{13}C{^{1}H}** (100 MHz) 156.6 (s), 136.8 (s), 131.7 (s), 129.2 (s), 128.5 (s), 127.6 (s), 127.1 (s), 124.0 (s), 120.7 (s), 111.8 (s), 69.8 (s, O*C*H_2), 30.6 (s, Se*C*H_2). **IR** (cm^{-1}, powder film): 3192 (m), 2914 (w), 2211 (m), 1645 (s), 1527 (s), 1210 (s), 1032 (s), 755 (s). HRMS (ESI) calcd for $C_{28}H_{27}O_2Se$ $[M - PdCl_2 + H]^+$: 475.1176, found 475.1118.

Procedure for Oxidative Annulation Reaction: A pressure tube was charged with 2-aryl imidazo[1,2-*a*]pyridine (0.250 mmol), 1,2-diarylethyne (1.1 equiv.), oxidant (2 equiv.), base (2 equiv.), and **3** (1.5 mol%) in 3 mL solvent. After that, the reaction mixture was refluxed at 110 °C for 16 h. The progress of reaction was monitored by TLC and reaction was quenched with aq. NH_4Cl. The reaction mixture was extracted with ethyl acetate (15 mL × 3). The crude product was purified by chromatography on silica-gel to afford annulated products **6a-6n** and **7o**.

Deuterium exchange experiment:

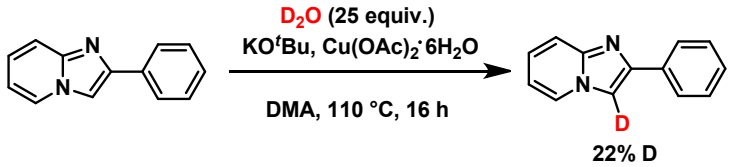

A 10 mL RBF was charged with 2-phenylimidazo[1,2-*a*]pyridine (1 equiv.), D_2O (25 equiv.), KO^{t}Bu (2 equiv.), $Cu(OAc)_2.6H_2O$ (2 equiv.), and DMA (3ml). The mixture was stirred at 110 °C under air for 16 h. The reaction mixture cooled to room temperature, quenched with water (5 mL) and diluted with EtOAc (15 mL). The layers were separated, and the aqueous layer was extracted with 3 x 10 mL of EtOAc. The organic layer is dried over Na_2SO_4, filtered, and concentrated on reduced pressure. The residue was purified by column chromatography on silica gel, eluting with 25-30% EtOAc /hexane. The isolated product was analyzed with ^{1}H NMR spectrometer and the result shown in figure s11.

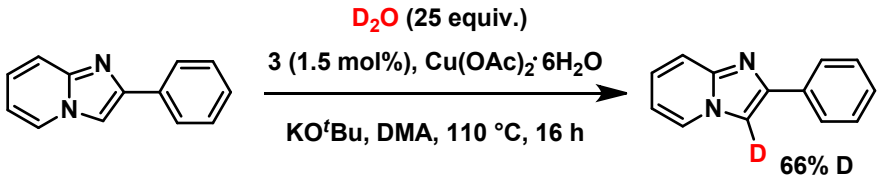

A 10 mL RBF was charged with 2-arylimidazo[1,2-*a*]pyridine (1 equiv.), D_2O (25 equiv.), KO^{t}Bu (2 equiv.), $Cu(OAc)_2.6H_2O$ (2 equiv.), **3** (1.5 mol %), and DMA (3ml). The mixture was stirred at 110 °C under air for 16 h. The reaction mixture cooled to room temperature, quenched with water (5 mL) and diluted with EtOAc (15 mL). The layers were separated, and the aqueous layer was extracted with 3 x 10 mL of EtOAc. The organic layer is dried over Na_2SO_4, filtered, and concentrated on reduced pressure. The residue was purified by column chromatography on silica gel, eluting with 25-30% EtOAc/hexane. The isolated product was analyzed with ^{1}H NMR spectrometer and the result shown in figure s12.

Crystallography

A. A CH_3CN solution of **3** (5 mL) was slowly concentrated over a period of 14 days to afford suitable colorless plate like crystals. The data was collected and reported in Table s1. Cell parameters were obtained from 60 data frames using a 1° scan and refined with 11864 reflections. APEX2 was used to collect the integrated intensity information of each reflection by reducing the data frames.[s1] Lorentz and polarization corrections were applied. The absorption correction program SADABS[s2] was employed to correct the data for absorption effects. The space group was determined from systematic reflection conditions and statistical tests. The structure was refined

(weighted least squares refinement on F^2) to convergence.[s3] Olex2[s4] was employed for the final data presentation and structure plots. Non-hydrogen atoms were refined with anisotropic thermal parameters. Hydrogen atoms were fixed in idealized positions using a riding model. The absence of additional symmetry or voids was confirmed using PLATON (ADDSYM).[s5] Molecule possess an inversion symmetry and symmetry generated atoms are not labeled in the Figure 1.

Table s1. Summary of crystallographic data.

	3
empirical formula	$C_{56}H_{52}Cl_2O_4PdSe_2$
formula weight	1124.19
temperature [K]	110.0
diffractometer	Bruker Apex 2
wavelength [Å]	0.71073
crystal system	Triclinic
space group	P-1
unit cell dimensions:	
a [Å]	8.2319(4)
b [Å]	10.9599(5)
c [Å]	14.1131(8)
α [°]	101.73(2)
β [°]	100.17(2)
γ [°]	97.03(2)
V [Å^3]	1210.44(11)
Z	1
ρ_{calc} [Mg/m^3]	1.542
μ [mm^{-1}]	2.044
F(000)	568
crystal size [mm^3]	0.10× 0.08 × 0.01
Θ limit [°]	2.548 to 25.000
index range (h, k, l)	–9, 9, –13, 12, –16, 16
reflections collected	11864
independent reflections	4210
R(int)	0.0273
completeness to θ	98.8
max. and min. transmission	0.3334 and 0.2686
data/restraints/parameters	4210/0/295
goodness-of-fit on F^2	1.060
R indices (final) [$I > 2\sigma(I)$]	
R_1	0.0253
wR_1	0.0491
R indices (all data)	
R_1	0.0352
wR_2	0.0547
largest diff. peak and hole [eÅ^{-3}]	0.471 and –0.363

Table s2. Key crystallographic distances [Å] and angles [°].

	3
Pd-Se1	2.4391(3)
Pd-Cl1	2.2869(6)
Se-C1	1.986(3)
Se-C15	1.984(2)
Cl-Pd-Se	87.85(17) 92.15(17)
Cl-Pd-Cl	180.0
Se-Pd-Se	180.0

The proposed dynamic process in 3 and calculation of barriers from experiment:

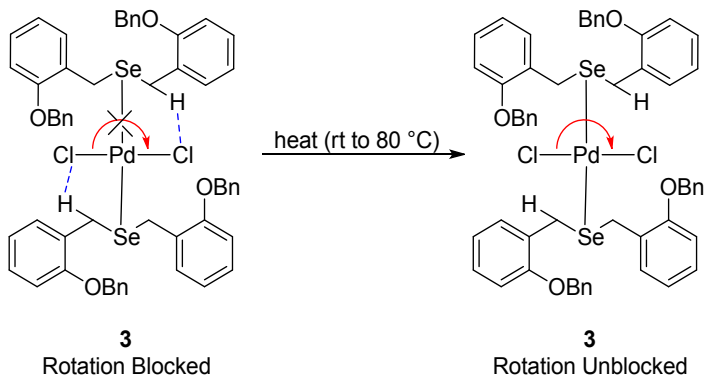

Scheme 1: The proposed dynamic process in **3**.

$\Delta G^{\ddagger} = \Delta H^{\ddagger} - T\Delta S^{\ddagger}$

$\Delta E^{\ddagger} \approx \Delta H^{\ddagger} - P\Delta V^{\ddagger}$

$P\Delta V^{\ddagger} \approx 0 \; and \; \Delta E^{\ddagger} \approx \Delta H^{\ddagger}$

$T\Delta S^{\ddagger} \approx 0$ Since the two hybrids stay exactly *trans* and the change in the number of degrees of freedom is approximately zero; therefore

$\Delta G^{\ddagger} = \Delta E^{\ddagger}$

Minimum rate (k_{min}) at 298.15 K is 26 s^{-1}.

$$k_{min} \leq \frac{k_B T}{h} e^{-\Delta E^{\ddagger}/RT} = k$$

$$26 \leq 2.08366179 * 10^{10} * 298.15 * e^{-\Delta E^{\ddagger}/(1.9872 * 298.15)}$$

$$\ln(26) \leq \ln\left(2.08366179 * 10^{10} * 298.15\right) - \frac{\Delta E^{\ddagger}}{(1.9872 * 298.15)}$$

$$3.25809653802 \leq 29.4575744674 - \frac{\Delta E^{\ddagger}}{(592.48368)}$$

$$(29.4575744674 - 3.25809653802) * (592.48368) \leq \Delta E^{\ddagger}$$

$$\Delta E^{\ddagger} \leq 15.52 \; kcal/mol$$

Table s3: Optimization of reaction conditions for cycloaromatization of 2-arylimidazo[1,2-*a*]pyridines (**4a**) with diphenylacetylene (**5a**)[a].

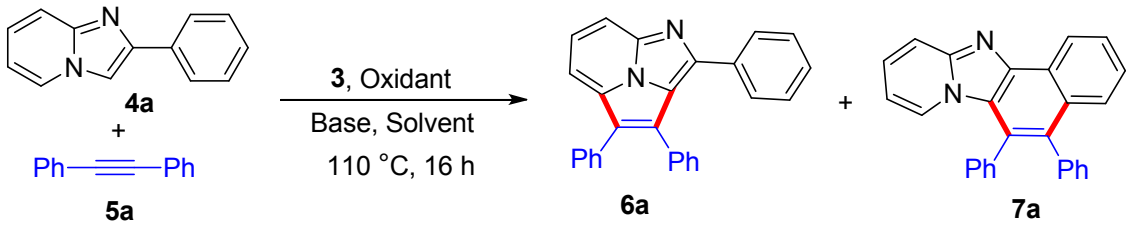

Entry no.	Catalyst (mol%)	Oxidant	Base	Solvent	Yield% (6a)[b]	Yield% (7a)[b]
1	**3** (1 mol%)	$Cu(OAc)_2.H_2O$	—	DMAc	31	nd
2	**3** (1 mol%)	$Cu(OAc)_2.H_2O$	K_2CO_3	DMAc	58	nd
3	**3** (1 mol%)	$Cu(OAc)_2.H_2O$	KO^{t}Bu	DMAc	67	nd
4	**3** (1 mol%)	$Cu(OAc)_2.H_2O$	K_3PO_4	DMAc	22	32
5	**3** (1 mol%)	$Cu(OAc)_2.H_2O$	Na_2CO_3	DMAc	11	nd
6	**3** (1 mol%)	$Cu(OAc)_2.H_2O$	DIPEA	DMAc	03	nd
7	**3** (1 mol%)	$AgNO_3$	KO^{t}Bu	DMAc	22	nd
8	**3** (1 mol%)	AgOAc	KO^{t}Bu	DMAc	52	nd
9	**3** (1 mol%)	Ag_2CO_3	KO^{t}Bu	DMAc	26	nd
10	**3** (1 mol%)	IBD	KO^{t}Bu	DMAc	21	27
11	**3** (1 mol%)	TBHP	KO^{t}Bu	DMAc	nr	nr
12	**3** (1 mol%)	$Cu(OAc)_2.H_2O$	KO^{t}Bu	DMF	36	23
13	**3** (1 mol%)	$Cu(OAc)_2.H_2O$	KO^{t}Bu	DMSO	54	19
14	**3** (1 mol%)	$Cu(OAc)_2.H_2O$	KO^{t}Bu	Xylene	08	nd
15	**3** (1.5 mol%)	$Cu(OAc)_2.H_2O$	KO^{t}Bu	DMAc	74	nd
16	**3** (2.0 mol%)	$Cu(OAc)_2.H_2O$	KO^{t}Bu	DMAc	63	13
17[c]	**3** (1.5 mol%)	$Cu(OAc)_2.H_2O$	KO^{t}Bu	DMAc	52	nd
18[d]	**3** (1.5 mol%)	$Cu(OAc)_2.H_2O$	KO^{t}Bu	DMAc	55	nd
19	**3** (1 mol%)	—	KO^{t}Bu	DMAc	nd	nd
20	—	$Cu(OAc)_2.H_2O$	KO^{t}Bu	DMAc	nd	nd
21[e]	**3** (1.5 mol%)	$Cu(OAc)_2.H_2O$	KO^{t}Bu	DMAc	13	nd

[a]Reaction conditions unless specified otherwise: **4a** (0.250 mmol), **5a** (1.1 equiv), oxidant (2 equiv), base (2 equiv), solvent (3 mL). nd = not determined, nr = no reaction. [b]Isolated yield. [c]at 90 °C. [d]at 10 h. [e]$Cu(OAc)_2.H_2O$ (10 mol%).

Computational Studies:

Initial geometry was taken from crystal structure **3** and optimized using QUICKSTEP module[s6] of CP2k program package.[s7] We used Perdew, Burke, and Ernzerhof (PBE) exchange–correlation functional (PBE XC functionals) and Goedecker-Teter-Hutter (GTH) pseudopotential[s8] with MOLOPT type DZVP basis set[s9] with an energy cut-off of 280 Ry. One of Cl-atom of optimized geometry **3** was further substituted as expected intermediate **A** to optimize *cis*- and *trans*- isomers. A visual inspection/representation was obtained using visual molecular dynamics program (VMD 1.9.2)[s10] and the distances between particular atom/ring and centre of mass of aromatic ring was drawn using Tcl scripting language embedded in VMD.

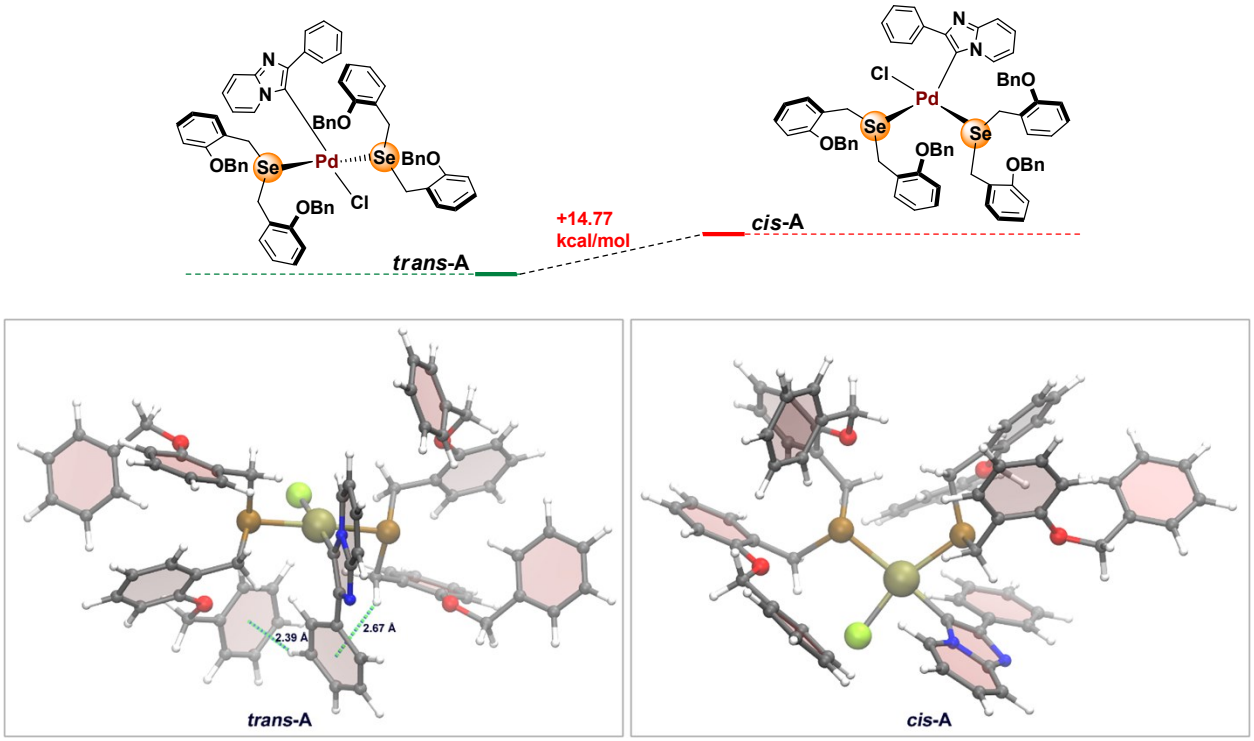

Figure s1: Geometry optimized structure of *trans*-**A** (CH-π distances 2.39 Å and 2.67 Å) and *cis*-**A** isomer. [Color scheme: Pd-Tan (CPK), Se-Ochre (CPK), Cl-Lime (CPK), C-Gray, H-White, N-Blue (Licorice); aromatic rings-Glass1 (Paperchain)]

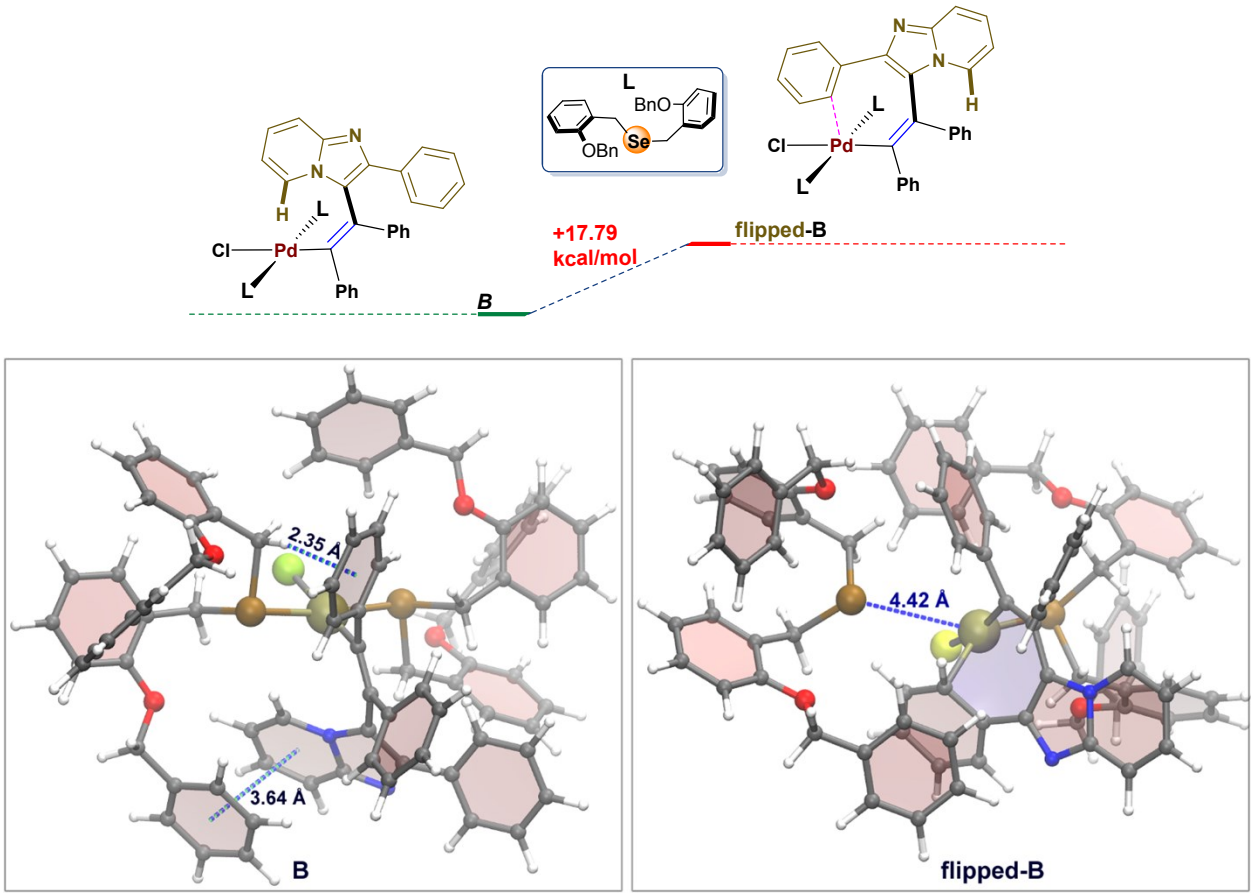

Figure s2: Geometry optimized structure of **B** (CH-π distance 2.35 Å and π-π distance 3.64 Å) and flipped-2-arylimidazo[1,2-*a*]pyridines of **B** (flipped-**B**). [Color scheme: Pd-Tan (CPK), Se-Ochre (CPK), Cl-Lime (CPK), C-Gray, H-White, N-Blue (Licorice); aromatic rings- Glass1 (Paperchain)]

In case of optimized structure of configuration **B**, CH-π interactions[s11] at distance 2.35 Å and π-π interactions at distance 3.64 Å are observed. Whereas, flipped-2-arylimidazo[1,2-*a*]pyridines of **B** optimization leads to 7 membered ring formation with breaking of Pd-Se bond having a distance of 4.42 Å. CH-π interactions and π-π interactions are not seen in between 2-arylimidazo[1,2-*a*]pyridines and **L** in **flipped-B** configuration of the complex and less favored with relatively higher energy i.e. 17.79 kcal/mol compared to configuration **B**.

Spectroscopic data of products:

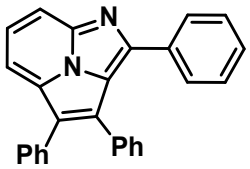

2,3,4-Triphenylimidazo[5,1,2-*cd*]indolizine (6a):[s12] Yellow solid, m.p: 208-210 ˚C; ^{1}H NMR (400 MHz, $CDCl_3$) δ 8.09 – 8.02 (m, 1H), 8.01 – 7.95 (m, 2H), 7.83 (d, *J* = 7.3 Hz, 2H), 7.47 (d, *J* = 7.3 Hz, 2H), 7.45 – 7.39 (m, 4H), 7.39 – 7.31 (m, 5H), 7.29 (d, *J* = 7.7 Hz, 2H); ^{13}C NMR (100 MHz, $CDCl_3$) δ 149.7 (s), 139.1 (s), 133.6 (s), 133.6 (s), 132.6 (s), 132.1 (s), 132.0 (s), 131.0 (s), 130.2 (s), 129.8 (s), 129.8 (s), 128.7 (s), 128.6 (s), 128.5 (s), 128.4 (s), 127.8 (s), 127.3 (s), 124.0 (s), 113.2 (s), 111.3 (s). HRMS (ESI) calcd for $C_{27}H_{19}N_2$ $[M + H]^+$: 371.1548, found 371.1594.

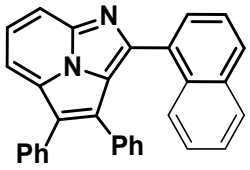

2-(Naphthalen-1-yl)-3,4-diphenylimidazo[5,1,2-*cd*]indolizine (6b):[s12] Yellow solid, m.p: 223-225 ˚C; ^{1}H NMR (400 MHz, $CDCl_3$) δ 8.20 (dd, *J* = 8.6, 1.7 Hz, 1H), 8.15 (s, 1H), 8.11 (dd, *J* = 6.6, 1.9 Hz, 1H), 8.06 – 8.00 (m, 2H), 7.86 – 7.81 (m, 2H), 7.56 – 7.47 (m, 6H), 7.47 – 7.38 (m, 6H), 7.38 – 7.32 (m, 1H). ^{13}C NMR (100 MHz, $CDCl_3$) δ 151.0 (s), 140.2 (s), 134.4 (s), 133.9 (s), 133.9 (s), 133.1 (s), 131.6 (s), 131.1 (s), 130.9 (s), 130.2 (s), 130.0 (s), 128.7 (s), 128.7 (s), 128.7 (s), 128.3 (s), 128.0 (s), 127.7 (s), 127.5 (s), 127.1 (s), 127.1 (s), 126.8 (s), 126.4 (s), 126.2 (s), 124.7 (s), 112.9 (s), 111.4 (s). (one carbon is not visible due to overlapping peaks)

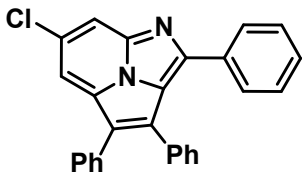

6-Chloro-2,3,4-triphenylimidazo[5,1,2-*cd*]indolizine (6c):[s12] Brown solid, m.p: 222-224 ˚C; ^{1}H NMR (400 MHz, $CDCl_3$) δ 8.18 (s, 1H), 7.94 (d, *J* = 7.3 Hz, 3H), 7.84 (s, 1H), 7.59 (d, *J* = 9.5 Hz, 2H), 7.45 (t, *J* = 7.6 Hz, 4H), 7.37 – 7.29 (m, 4H).7.15 (d, *J* = 9.4 Hz, 2H). ^{13}C NMR (100 MHz, $CDCl_3$) δ 149.5 (s), 139.9 (s), 133.9 (s), 133.7 (s), 132.6 (s), 131.8 (s), 131.5 (s), 131.0 (s), 130.9 (s), 130.1 (s), 128.7 (s), 128.3 (s), 127.7 (s), 127.2 (s), 127.1 (s), 124.3 (s), 123.8 (s), 113.0 (s), 111.6 (s).

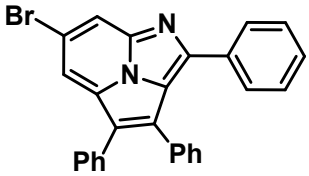

6-Bromo-2,3,4-triphenylimidazo[5,1,2-cd]indolizine (6d): Light brown solid, m.p: 235-237 ˚C; ^{1}H NMR (400 MHz, $CDCl_3$) 8.11 – 8.06 (m, 1H), 8.04 – 8.00 (m, 2H), 7.71 (d, *J* = 8.5 Hz, 2H), 7.53 – 7.47 (m, 3H), 7.47 – 7.38 (m, 8H), 7.38 – 7.32 (m, 1H). ^{13}C NMR (100 MHz, $CDCl_3$) δ 149.82 (s), 140.25 (s), 134.21 (s), 134.03 (s), 132.90 (s), 132.11 (s), 131.86 (s), 131.80

(s), 131.36 (s), 131.20 (s), 130.44 (s), 128.98 (s), 128.66 (s), 127.98 (s), 127.56 (s), 127.46 (s), 124.13 (s), 113.35 (s), 111.91 (s).

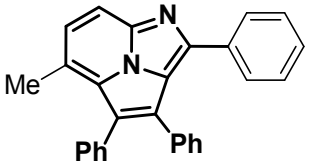

5-Methyl-2,3,4-triphenylimidazo[5,1,2-*cd*]indolizine (6e): Yellow solid, m.p: 184-186 ˚C; ^{1}H NMR (400 MHz, $CDCl_3$) δ δ 7.92 – 7.76 (m, 4H), 7.51 – 7.26 (m, 13H), 2.85 (s, 3H); ^{13}C NMR (100 MHz, $CDCl_3$) δ 150.8 (s), 139.9 (s), 138.6 (s), 134.1 (s), 134.1 (s), 133.7 (s), 131.8 (s), 131.3 (s), 131.0 (s), 130.2 (s), 129.6 (s), 129.3 (s), 128.6 (s), 128.5 (s), 128.3 (s), 127.0 (s), 126.7 (s), 123.9 (s), 113.8 (s), 111.9 (s), 22.9 (s).

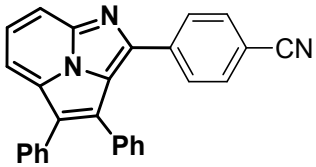

4-(3,4-Diphenylimidazo[5,1,2-*cd*]indolizin-2-yl)benzonitrile (6f): Orange solid, m.p: 238-240 ˚C; ^{1}H NMR (400 MHz, $CDCl_3$) δ 8.14 – 8.09 (m, 1H), 8.04 (d, J = 4.3 Hz, 2H), 7.90 (d, J = 8.1 Hz, 2H), 7.55 (d, J = 8.1 Hz, 2H), 7.50 – 7.31 (m, 10H); ^{13}C NMR (100 MHz, $CDCl_3$) δ 147.5 (s), 139.6 (s), 137.7 (s), 133.4 (s), 133.1 (s), 131.8 (s), 131.8 (s), 131.2 (s), 130.5 (s), 129.8 (s), 129.6 (s), 128.5 (s), 128.4 (s), 128.3 (s), 128.2 (s), 127.3 (s), 127.1 (s), 124.6 (s), 118.5 (s), 113.4 (s), 112.2 (s), 112.1 (s).

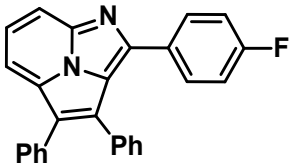

2-(4-Fluorophenyl)-3,4-diphenylimidazo[5,1,2-*cd*]indolizine (6g):[s12] Yellow solid, m.p: 203-205 ˚C; ^{1}H NMR (400 MHz, $CDCl_3$) δ 8.14 (d, J = 6.6 Hz, 1H), 8.08 – 8.00 (m, 2H), 7.84 (q, J = 8.6, 5.5 Hz, 2H), 7.51 – 7.33 (m, 10H), 7.00 (t, J = 8.6 Hz, 2H); ^{13}C NMR (100 MHz, $CDCl_3$) δ 163.8 (d, J_{C-F} = 258.8 Hz), 149.0 (s), 139.3 (s), 133.8 (s), 133.6 (d, J_{C-F} = 17.7 Hz), 131.9 (s), 131.8 (s), 131.7 (d, J_{C-F} = 8.4 Hz) , 130.9 (s), 130.1 (s), 128.7 (s), 128.6 (s), 128.4 (s), 127.6 (s), 127.2 (s), 115.5 (d, J_{C-F} = 21.6 Hz), 113.1 (s), 111.2 (s).

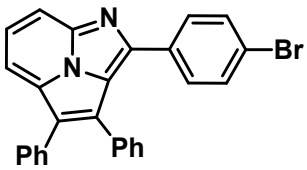

2-(4-Bromophenyl)-3,4-diphenylimidazo[5,1,2-*cd*]indolizine (6h): Yellow solid, m.p: 221-223 ˚C; ^{1}H NMR (400 MHz, $CDCl_3$) δ 8.08 – 8.03 (m, 1H), 8.02 – 7.97 (m, 2H), 7.69 (d, J = 8.5 Hz, 2H), 7.50 – 7.29 (m, 12H); ^{13}C NMR (100 MHz, $CDCl_3$) δ 149.5 (s), 140.0 (s), 133.9 (s), 133.7 (s), 132.6 (s), 131.8 (s), 131.6 (s), 131.0 (s), 130.9 (s), 130.1 (s), 128.7 (s), 128.4 (s), 127.7 (s), 127.2 (s), 127.2 (s), 123.8 (s), 113.0 (s), 111.6 (s).

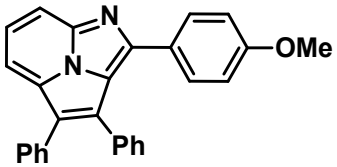

2-(4-Methoxyphenyl)-3,4-diphenylimidazo[5,1,2-*cd*]indolizine (6i):[s12] Pale yellow solid, m.p: 198-200 ˚C; ^{1}H NMR (400 MHz,

$CDCl_3$) δ 8.16 (d, J = 7.4 Hz, 1H), 8.09 – 7.97 (m, 2H), 7.84 (d, J = 8.5 Hz, 2H), 7.52 – 7.34 (m, 10H), 6.85 (d, J = 8.4 Hz, 2H), 3.86 (s, 3H); ^{13}C NMR (100 MHz, $CDCl_3$) δ 160.8 (s), 147.6 (s), 140.2 (s), 134.2 (s), 134.1 (s), 131.5 (s), 131.4 (s), 131.1 (s), 131.0 (s), 130.2 (s), 128.6 (s), 128.5 (s), 128.1 ()s, 126.9 (s), 126.8 (s), 126.3 (s), 113.8 (s), 112.4 (s), 110.6 (s), 55.3 (s).

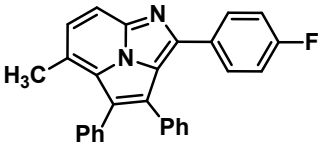

2-(4-Fluorophenyl)-5-methyl-3,4-diphenylimidazo[5,1,2-*cd*]indolizine (6j): Light brown solid, m.p: 184-186 ˚C; ^{1}H NMR (400 MHz, $CDCl_3$) δ 7.98 (d, J = 8.1 Hz, 1H), 7.82 (dd, J = 8.6, 5.5 Hz, 2H), 7.74 (d, J = 8.1 Hz, 1H), 7.48 – 7.22 (m, 10H), 6.99 (t, J = 8.7 Hz, 2H), 2.56 (s, 3H); ^{13}C NMR (100 MHz, $CDCl_3$) δ 163.6 (d, J_{C-F} = 247.9 Hz), 148.1 (s), 138.2 (s), 134.1 (s), 133.6 (s), 131.9 (s), 131.5 (d, J_{C-F} = 7.4 Hz), 131.4 (s), 131.1 (s), 130.0 (d, J_{C-F} = 7.0 Hz), 129.9 (s), 128.2 (s), 128.0 (s), 127.9 (s), 127.5 (s), 125.6 (s), 123.5 (s), 115.4 (d, J_{C-F} = 21.5 Hz), 111.0 (s), 17.8 (s).

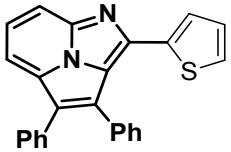

3,4-Diphenyl-2-(thiophen-2-yl)imidazo[5,1,2-*cd*]indolizine (6k):[s12] Brown solid, m.p: 209-211 ˚C; ^{1}H NMR (400 MHz, $CDCl_3$) δ 8.03 – 7.95 (m, 3H), 7.56 – 7.51 (m, 2H), 7.50 – 7.45 (m, 5H), 7.44 – 7.31 (m, 4H), 7.00 (dd, J = 3.7, 0.9 Hz, 1H), 6.96 – 6.92 (m, 1H); ^{13}C NMR (100 MHz, $CDCl_3$) δ 144.9 (s), 140.0 (s), 137.7 (s), 134.1 (s), 133.8 (s), 131.5 (s), 131.1 (s), 130.8 (s), 130.0 (s), 129.1 (s), 128.7 (s), 128.6 (s), 128.5 (s), 128.4 (s), 128.0 (s), 127.5 (s), 127.2 (s), 127.0 (s), 123.4 (s), 112.8 (s), 111.0 (s).

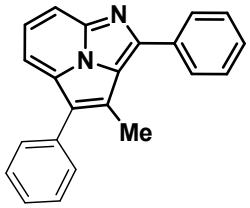

3-Methyl-2,4-diphenylimidazo[5,1,2-*cd*]indolizine (6l):[s12] Yellow solid, m.p: 115-117 ˚C; ^{1}H NMR (400 MHz, $CDCl_3$) δ 8.33 – 8.28 (m, 2H), 7.98 (d, J = 8.0 Hz, 1H), 7.91 (t, J = 7.6 Hz, 1H), 7.84 (d, J = 7.6 Hz, 1H), 7.69 – 7.64 (m, 2H), 7.62 – 7.55 (m, 4H), 7.52 – 7.42 (m, 2H), 2.93 (s, 3H); ^{13}C NMR (100 MHz, $CDCl_3$) δ 150.3 (s), 139.8 (s), 134.4 (s), 134.1 (s), 132.0 (s), 130.0 (s), 129.4 (s), 129.1 (s), 128.9 (s), 128.9 (s), 128.6 (s), 127.5 (s), 127.2 (s), 126.7 (s), 111.3 (s), 110.6 (s), 14.0 (s).

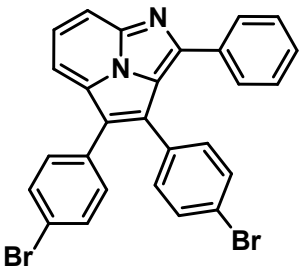

3,4-Bis(4-bromophenyl)-2-phenylimidazo[5,1,2-*cd*]indolizine (6m): Yellow solid, m.p: 200-202 ˚C; ^{1}H NMR (400 MHz, $CDCl_3$) δ 8.09 (d, J = 7.7 Hz, 1H), 8.03 – 7.92 (m, 2H), 7.83 (d, J = 7.4 Hz, 2H), 7.59 – 7.48 (m, 4H), 7.44 – 7.25 (m, 7H); ^{13}C NMR (100 MHz, $CDCl_3$) δ 151.5 (s), 140.1 (s), 133.4 (s), 132.6 (s), 132.57 (s), 132.1 (s), 131.9 (s), 131.7

(s), 131.3 (s), 130.1 (s), 129.7 (s), 129.67 (s), 128.5 (s), 127.3 (s), 126.0 (s), 123.8 (s), 122.8 (s), 121.6 (s), 112.7 (s), 111.8 (s).

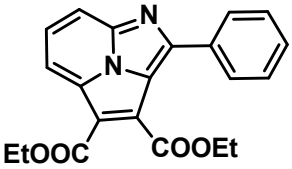

Diethyl 2-phenylimidazo[5,1,2-*cd*]indolizine-3,4-dicarboxylate (6n): Yellow solid, m.p: 119-121 ˚C; ^{1}H NMR (400 MHz, $CDCl_3$) δ 8.42 – 8.35 (m, 1H), 8.26 (d, *J* = 7.8 Hz, 2H), 8.16 – 8.09 (m, 2H), 7.63 – 7.50 (m, 3H), 4.60 (q, *J* = 7.1 Hz, 2H), 4.53 (q, *J* = 7.1 Hz, 2H), 1.51 (t, *J* = 7.1 Hz, 3H), 1.45 (t, *J* = 7.1 Hz, 3H); ^{13}C NMR (100 MHz, $CDCl_3$) δ 165.6 (s), 163.3 (s), 154.6 (s), 140.9 (s), 132.9 (s), 130.8 (s), 130.1 (s), 129.4 (s), 129.1 (s), 129.1 (s), 116.4 (s), 116.2 (s), 112.7 (s), 62.7 (s), 61.1 (s), 14.4 (s), 14.1 (s).

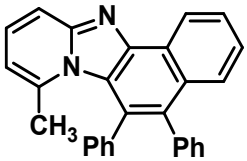

8-Methyl-5,6-diphenylnaphtho[1',2':4,5]imidazo[1,2-*a*]pyridine (7o):[s12] Yellow solid, m.p: 271-273 ˚C; ^{1}H NMR (400 MHz, $CDCl_3$) δ 8.10 (d, *J* = 8.0 Hz, 1H), 8.02 (d, *J* = 8.0 Hz, 2H), 7.77 (s, 3H), 7.64 – 7.51 (m, 3H), 7.47 (t, *J* = 7.7 Hz, 4H), 7.41 – 7.31 (m, 3H), 6.74 (d, *J* = 7.7 Hz, 1H), 2.67 (s, 3H); ^{13}C NMR (100 MHz, $CDCl_3$) δ 139.6 (s), 137.9 (s), 134.0 (s), 131.6 (s), 131.6 (s), 131.0 (s), 130.2 (s), 129.6 (s), 129.1 (s), 129.1 (s), 128.6 (s), 128.5 (s), 128.1 (s), 127.0 (s), 126.9 (s), 123.3 (s), 120.8 (s), 114.8 (s), 112.6 (s), 112.2 (s), 111.0 (s), 29.7 (s).

Copies of spectral data

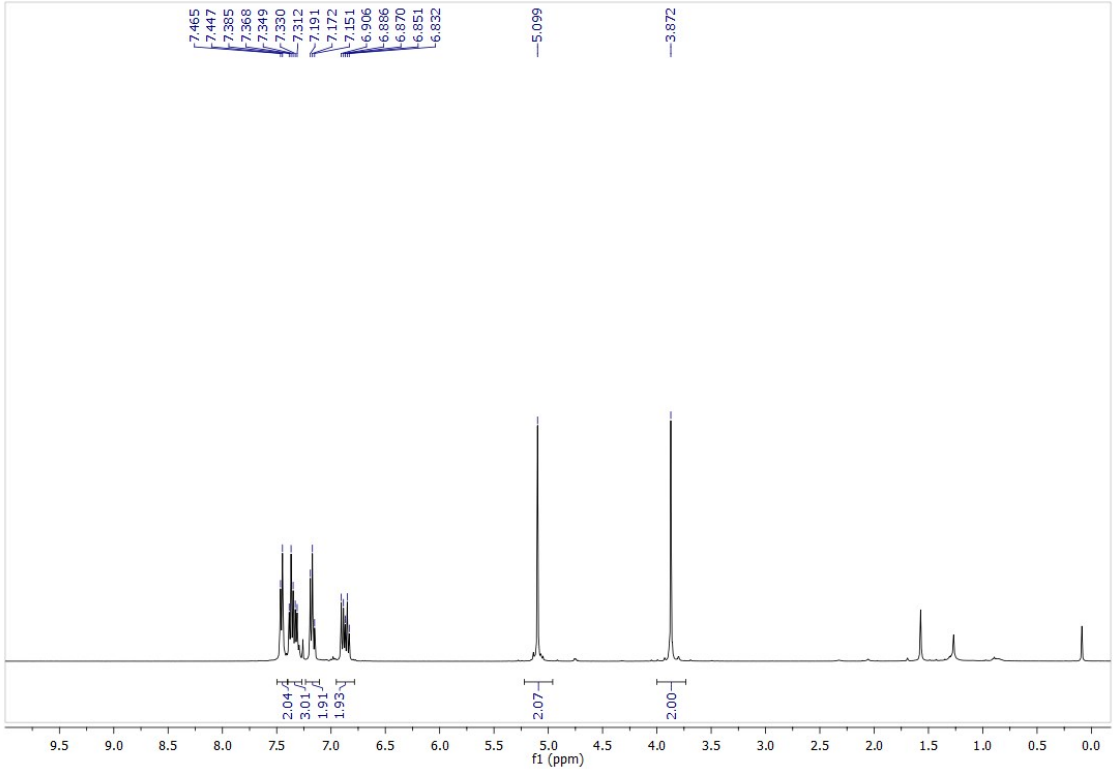

Figure s3. ^{1}H NMR spectrum of **2**.

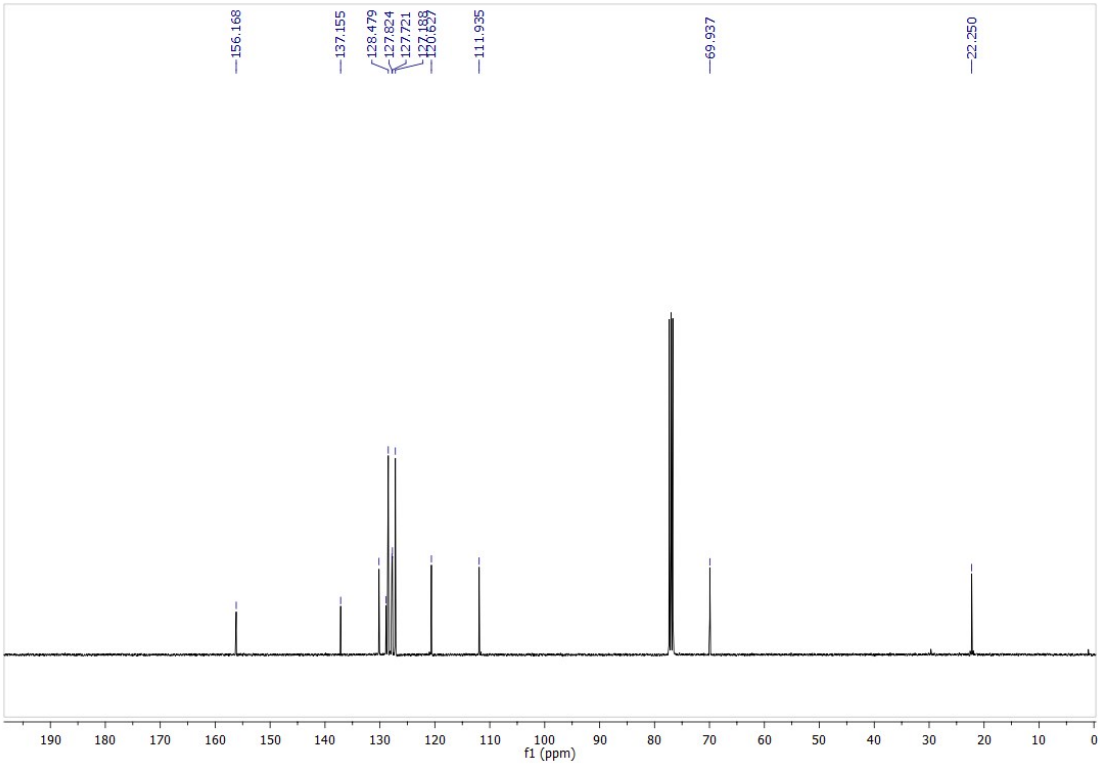

Figure s4. ^{13}C{^{1}H} NMR spectrum of **2**.

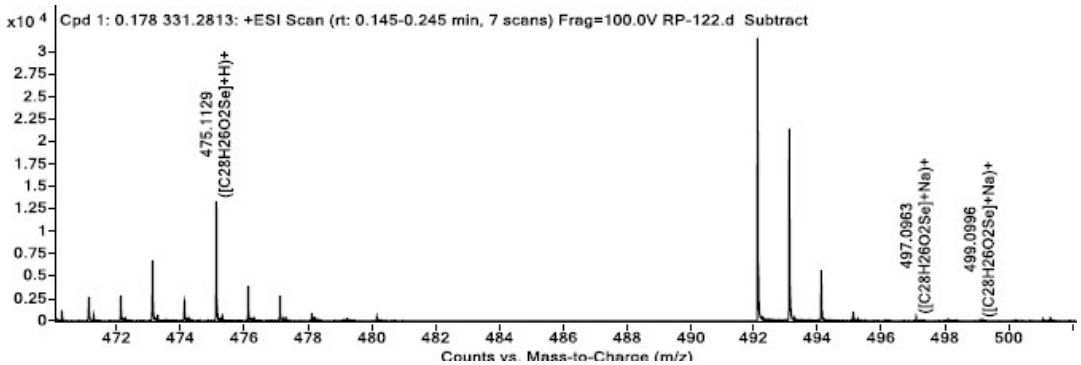

Figure s5. HRMS of **2**.

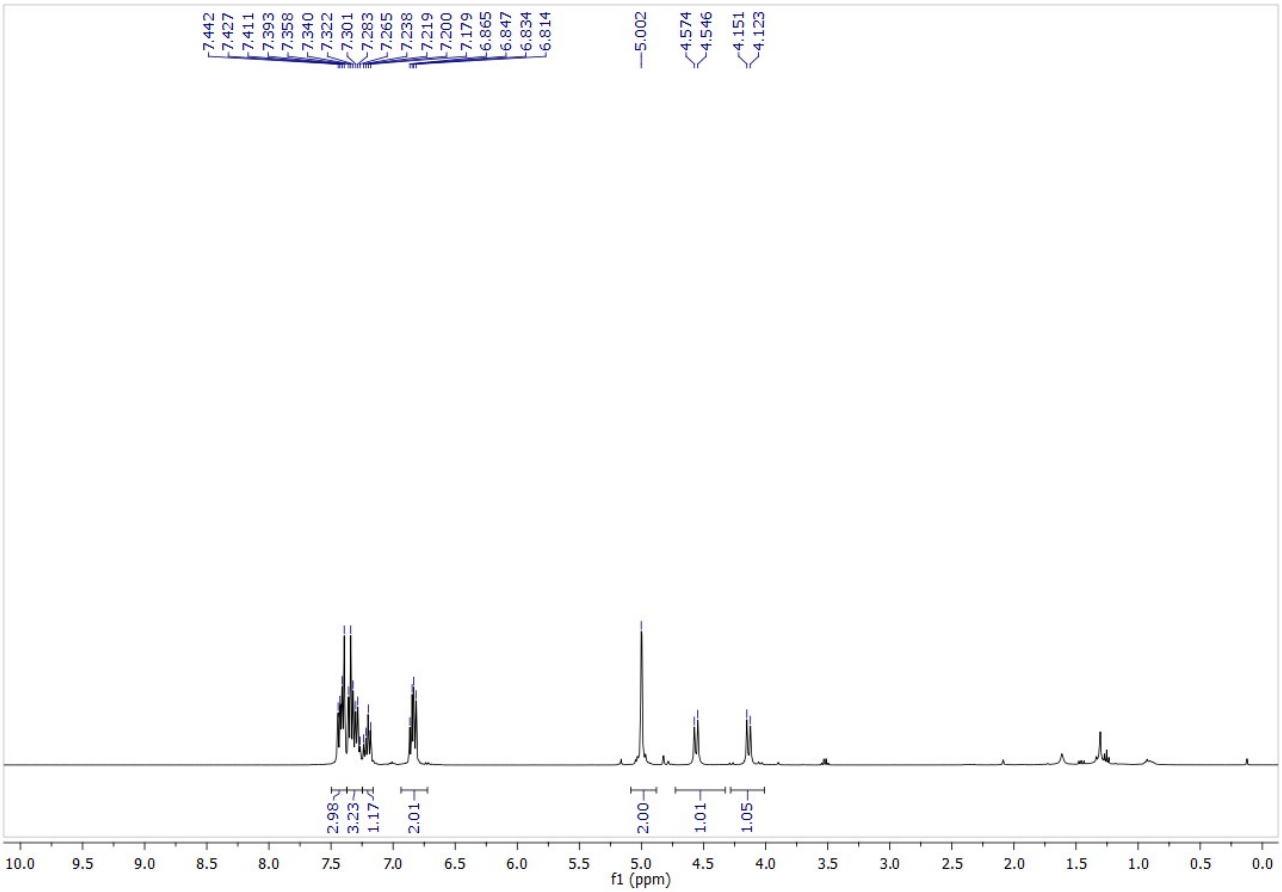

Figure s6. ^{1}H NMR spectrum of **3**.

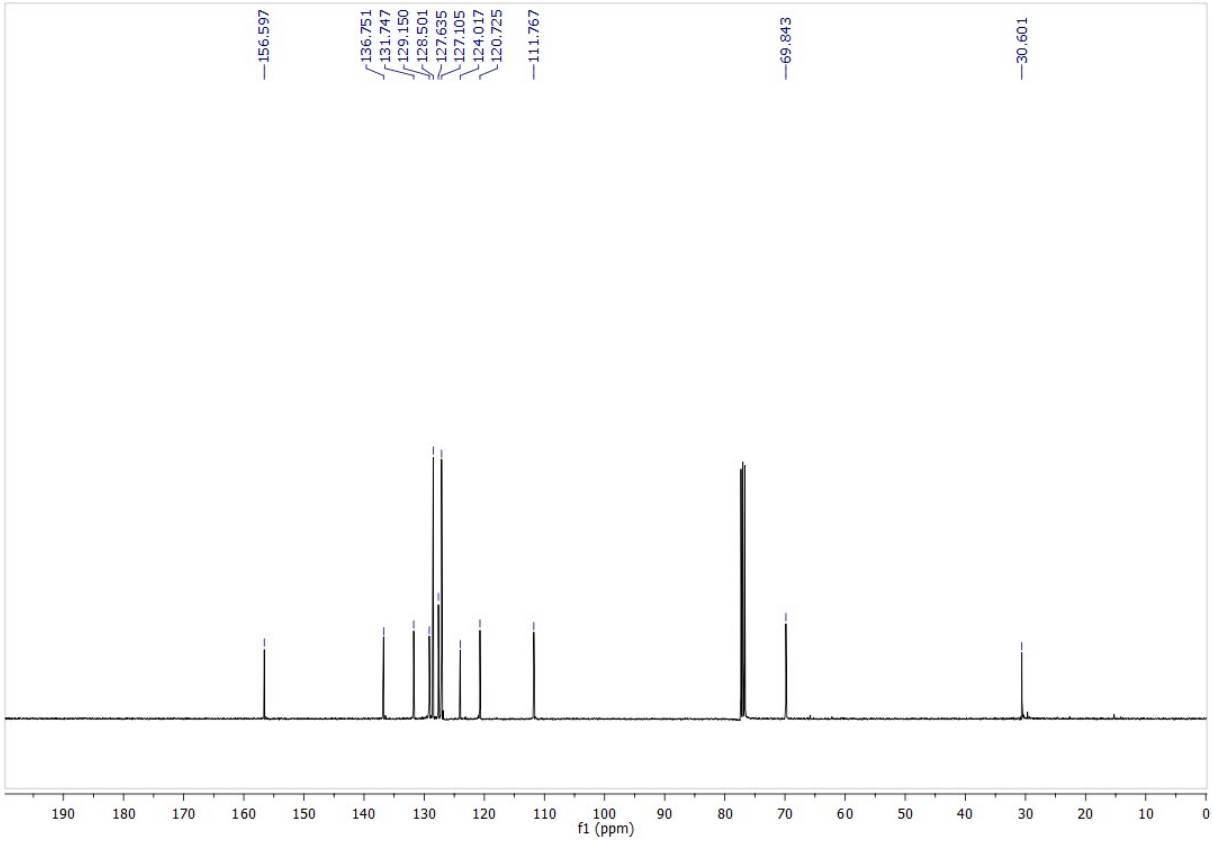

Figure s7. $^{13}C\{^{1}H\}$ NMR spectrum of **3**.

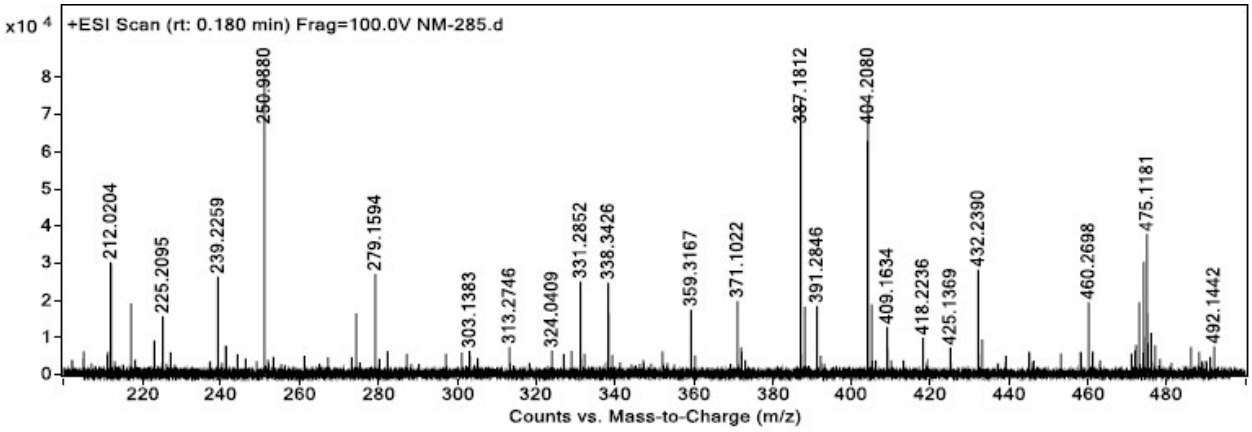

Figure s8. HRMS of **3**.

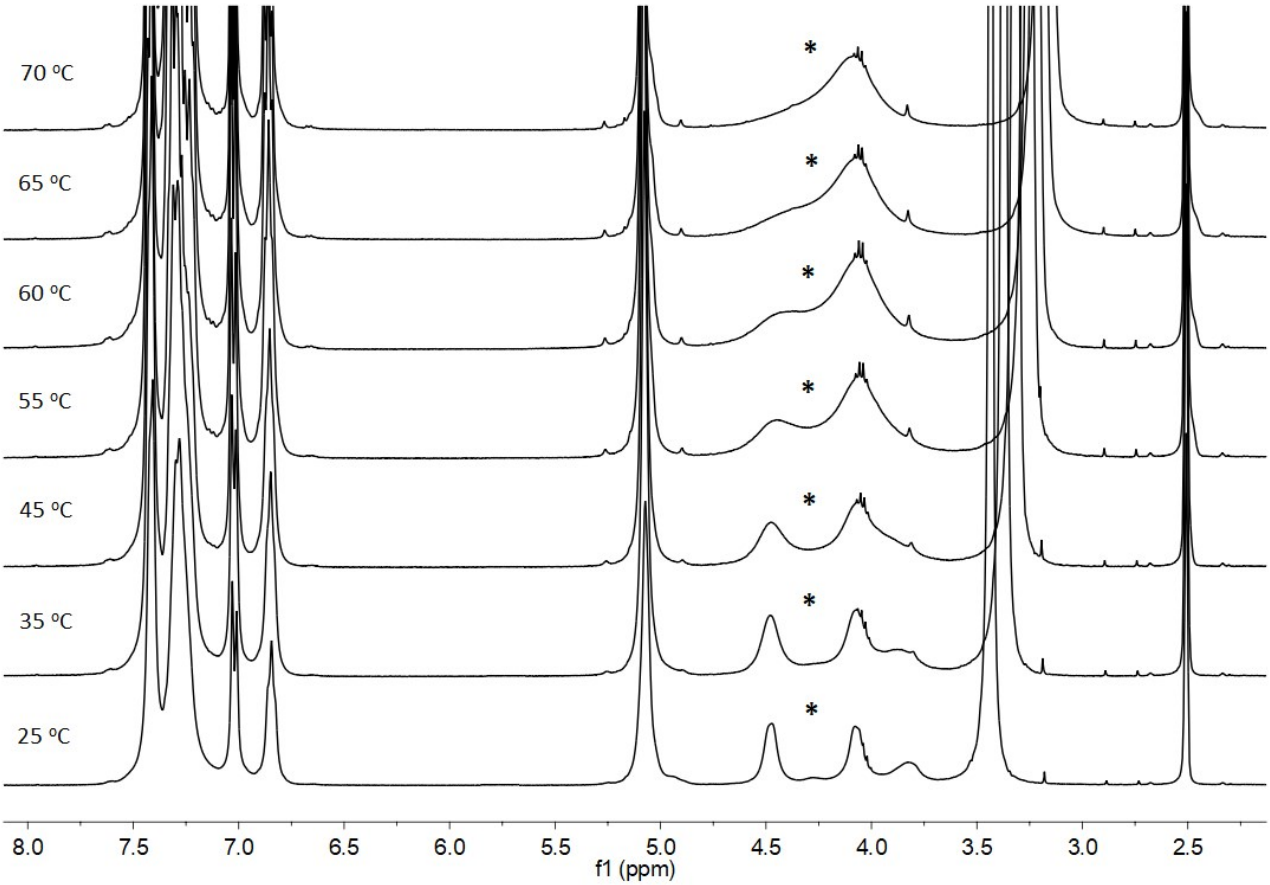

Figure s9. ^{1}H NMR spectra of **3** as a function of temperature (DMSO-d_6): Coalescing signals are denoted with a *.

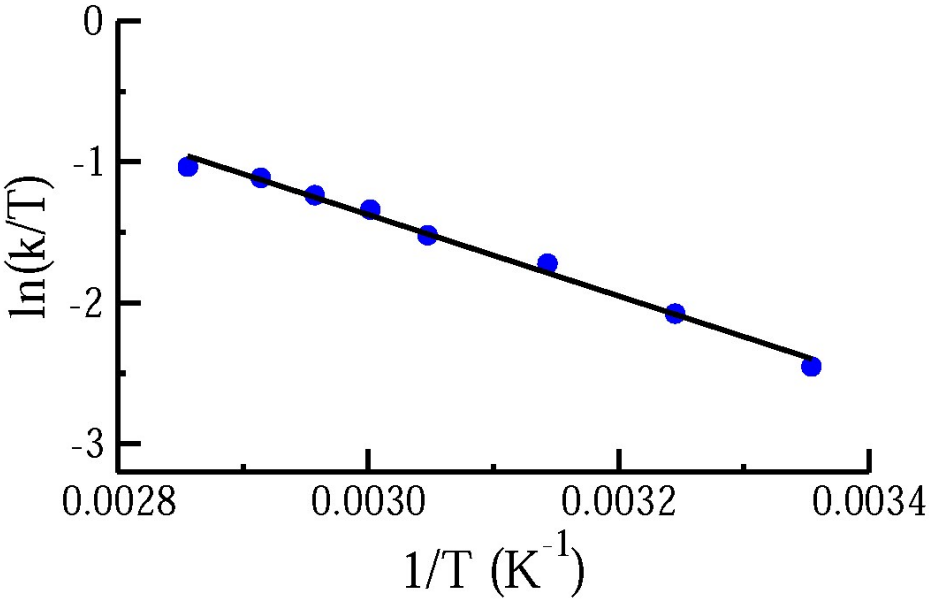

Figure s10. Eyring plot using rate constants derived from Figure 3 for the dynamic process of **3**.

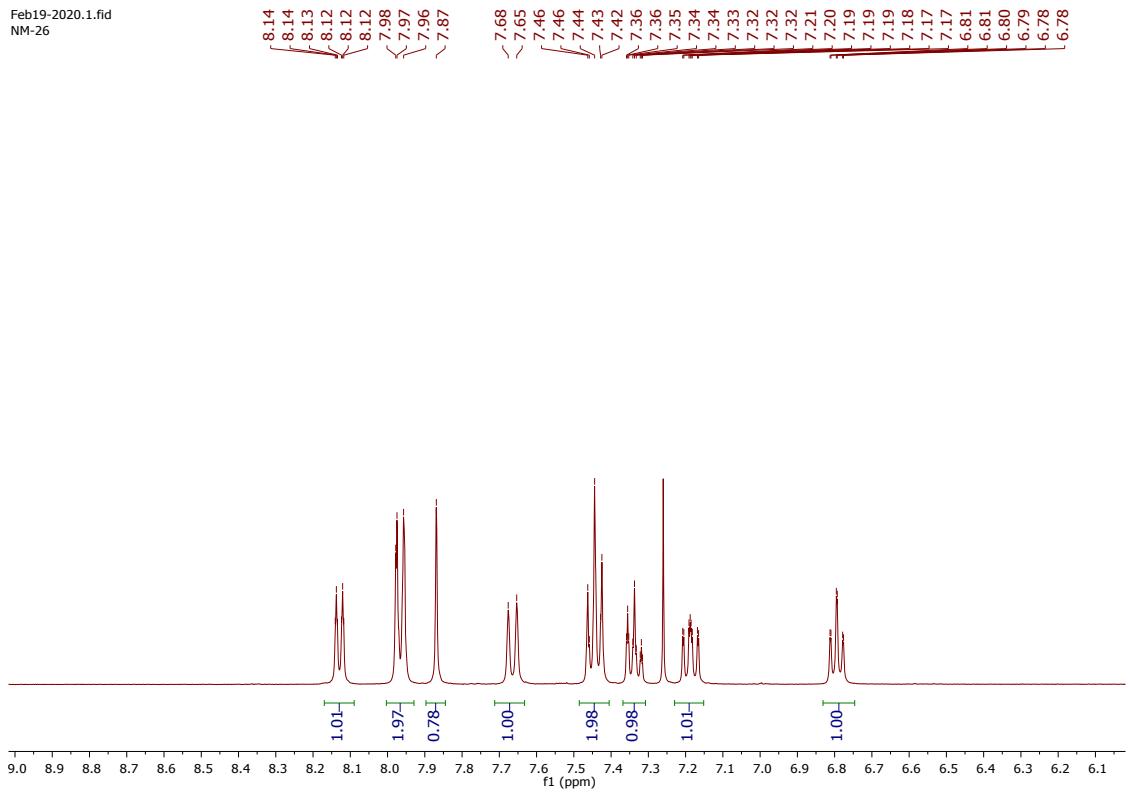

Figure s11. ^{1}H NMR spectrum of deuterium exchange experiment in absence of catalyst.

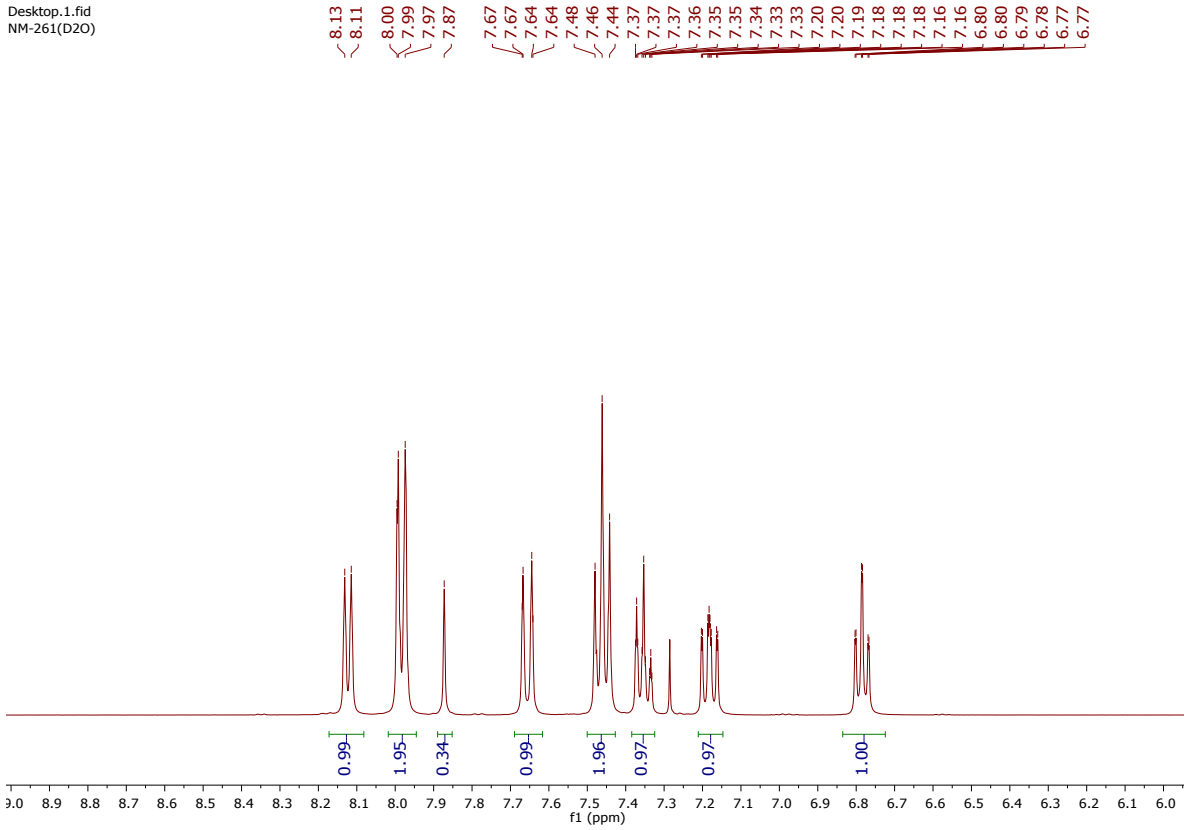

Figure s12. ^{1}H NMR spectrum of deuterium exchange experiment in presence of catalyst.

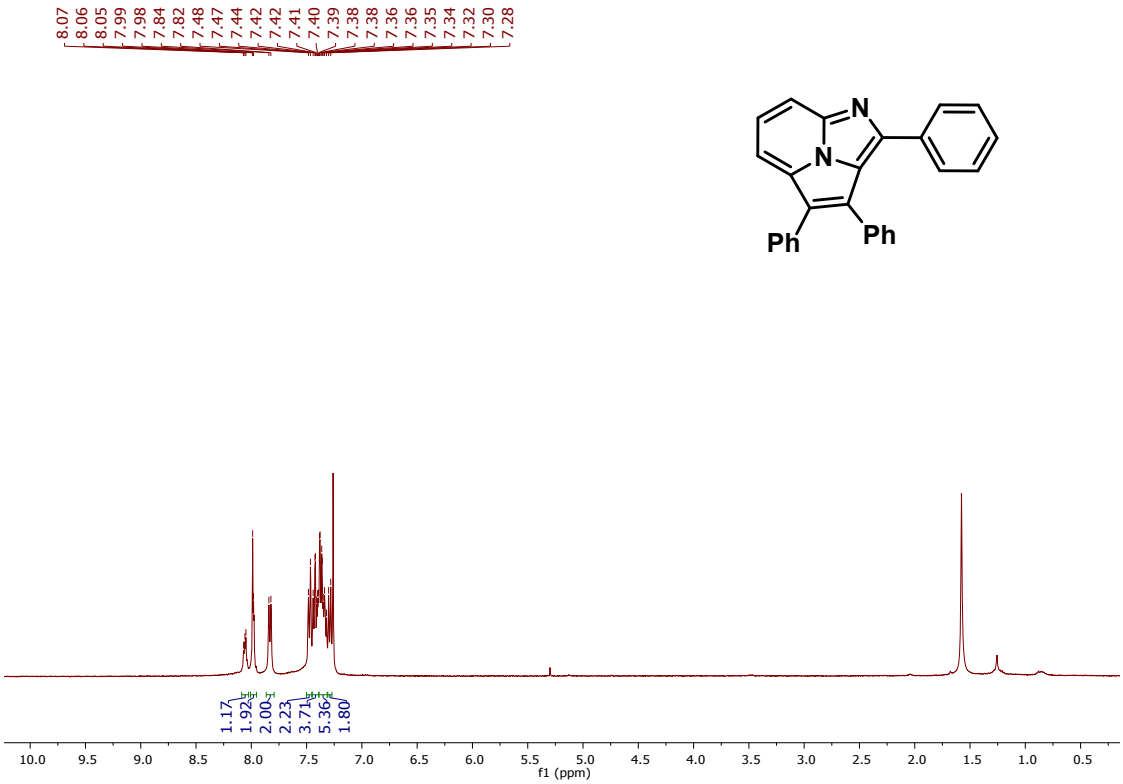

Figure s13. ^{1}H NMR spectrum of **6a**.

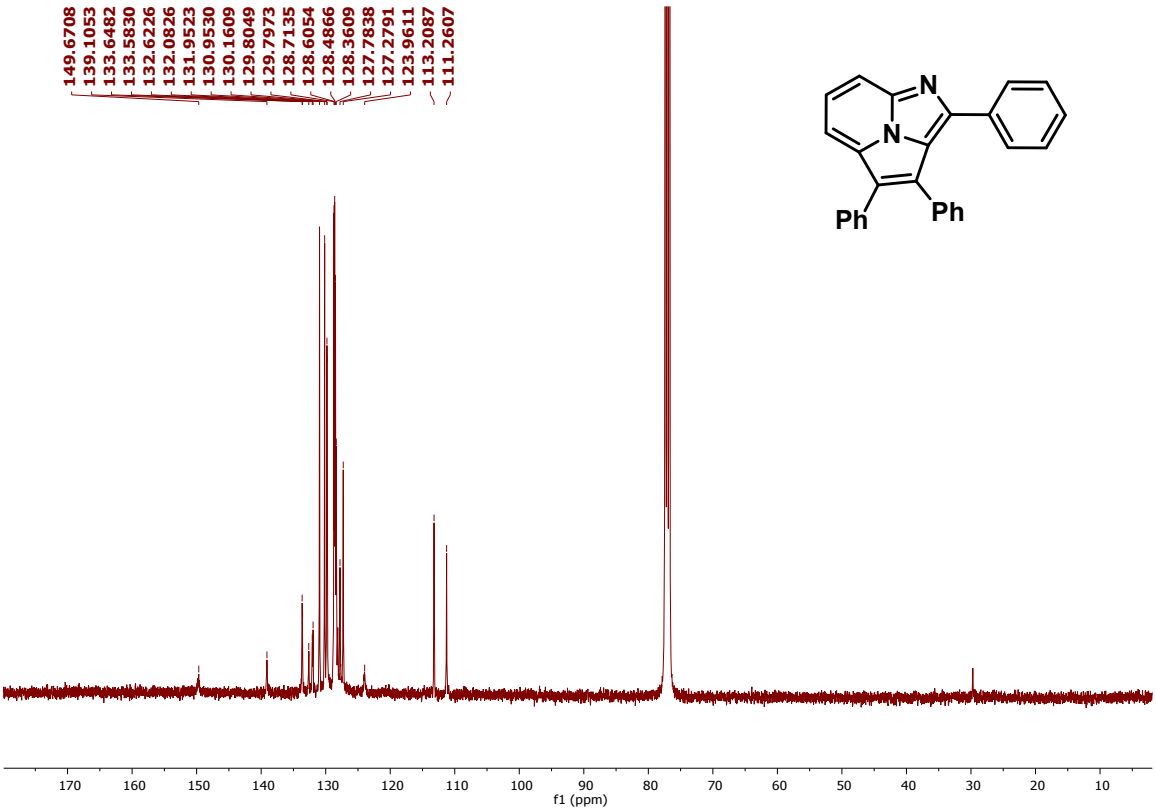

Figure s14. ^{13}C{^{1}H} NMR spectrum of **6a**.

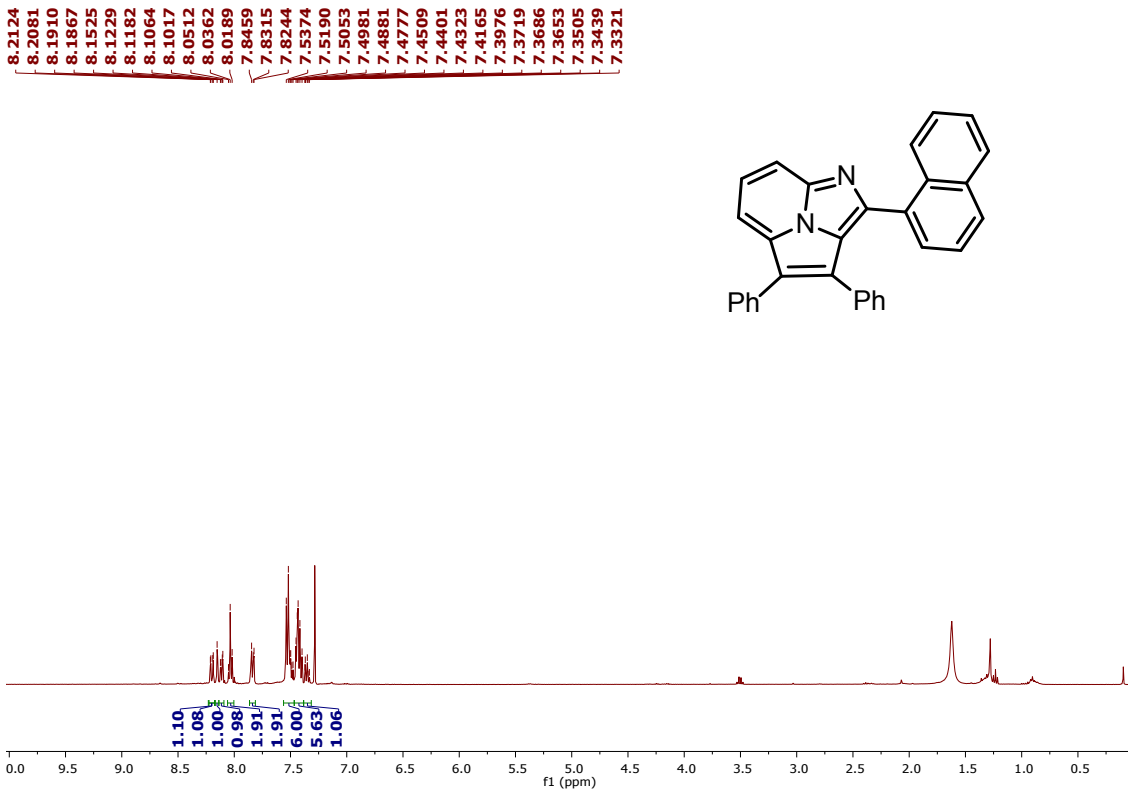

Figure s15. ^{1}H NMR spectrum of **6b**.

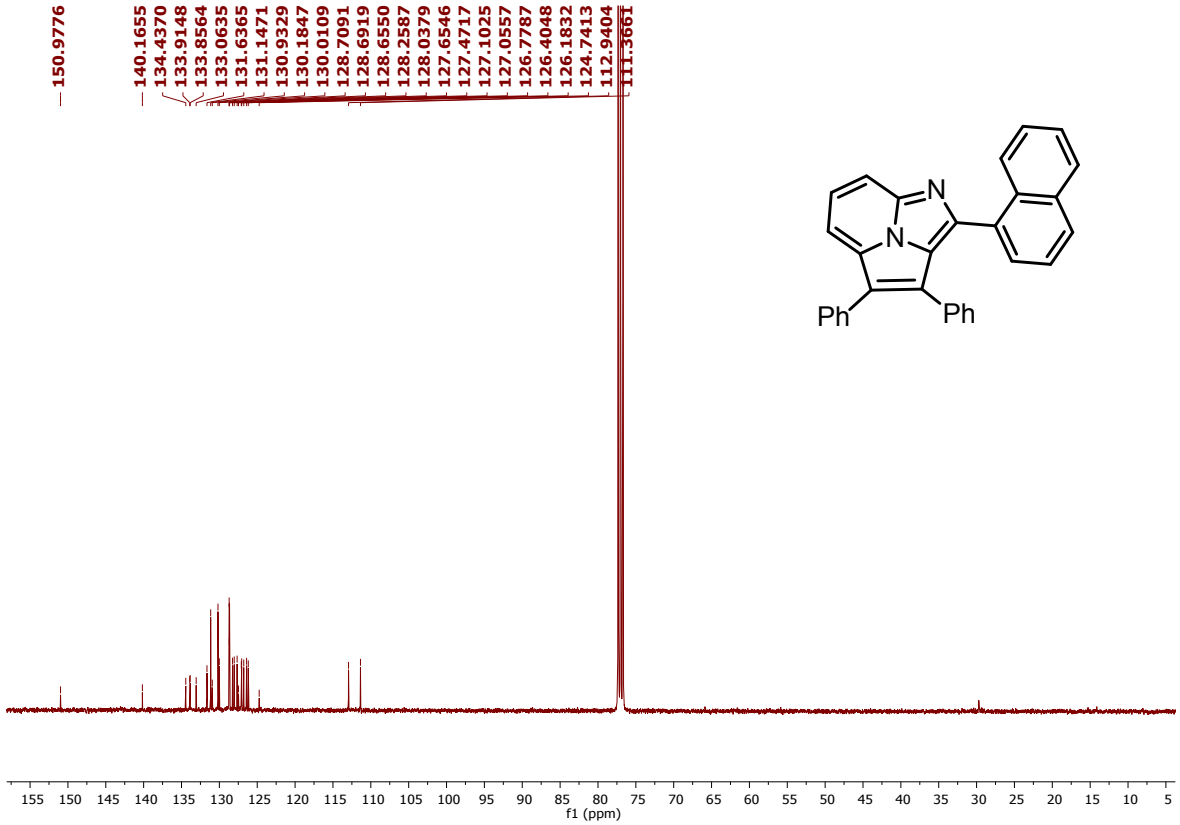

Figure s16. ^{13}C{^{1}H} NMR spectrum of **6b**.

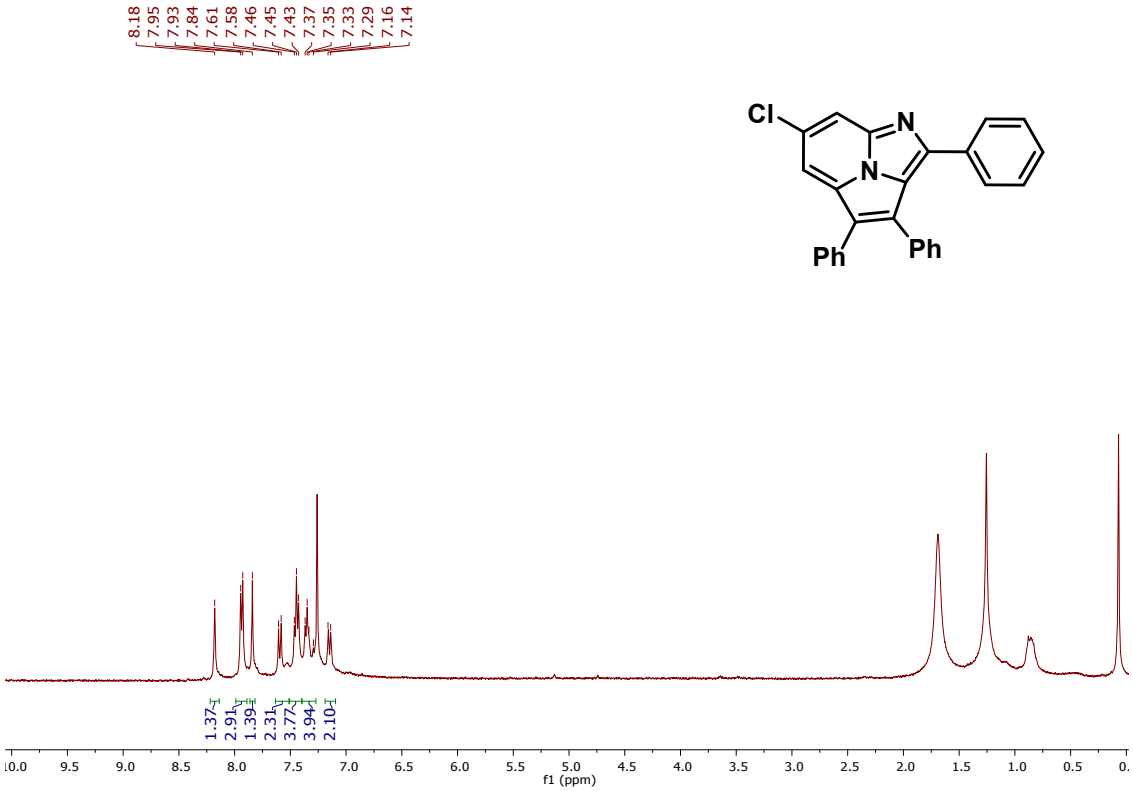

Figure s17. ^{1}H NMR spectrum of **6c**.

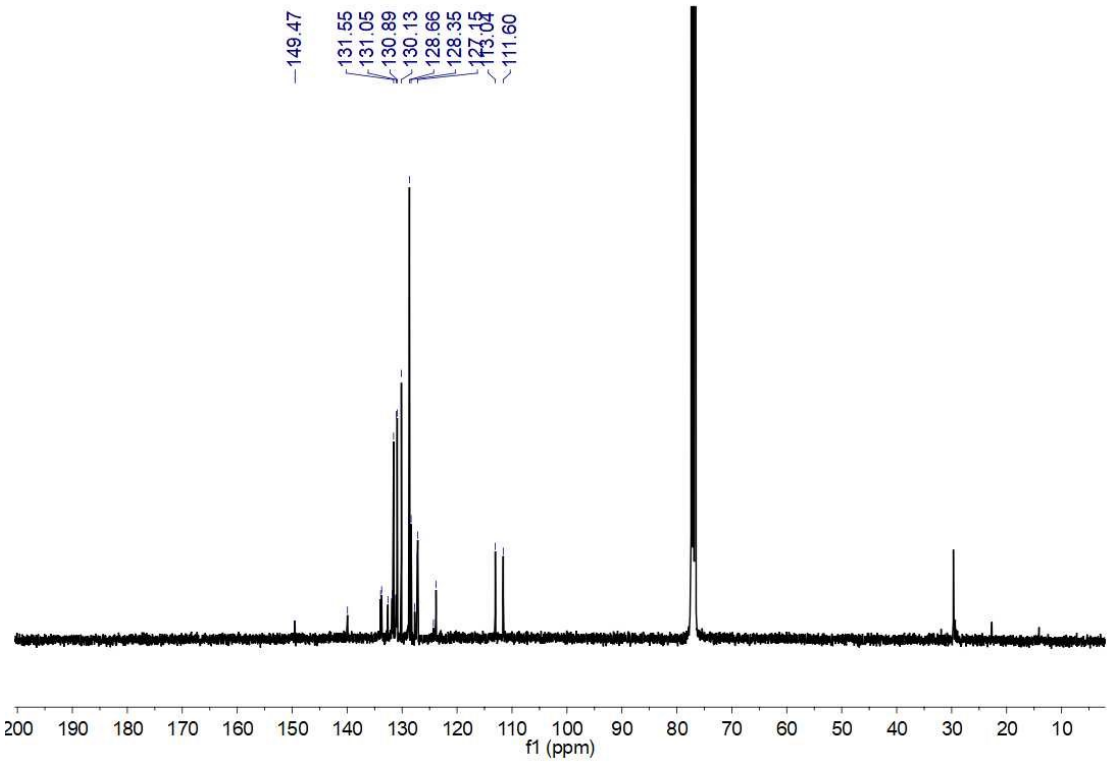

Figure s18. ^{13}C{^{1}H} NMR spectrum of **6c**.

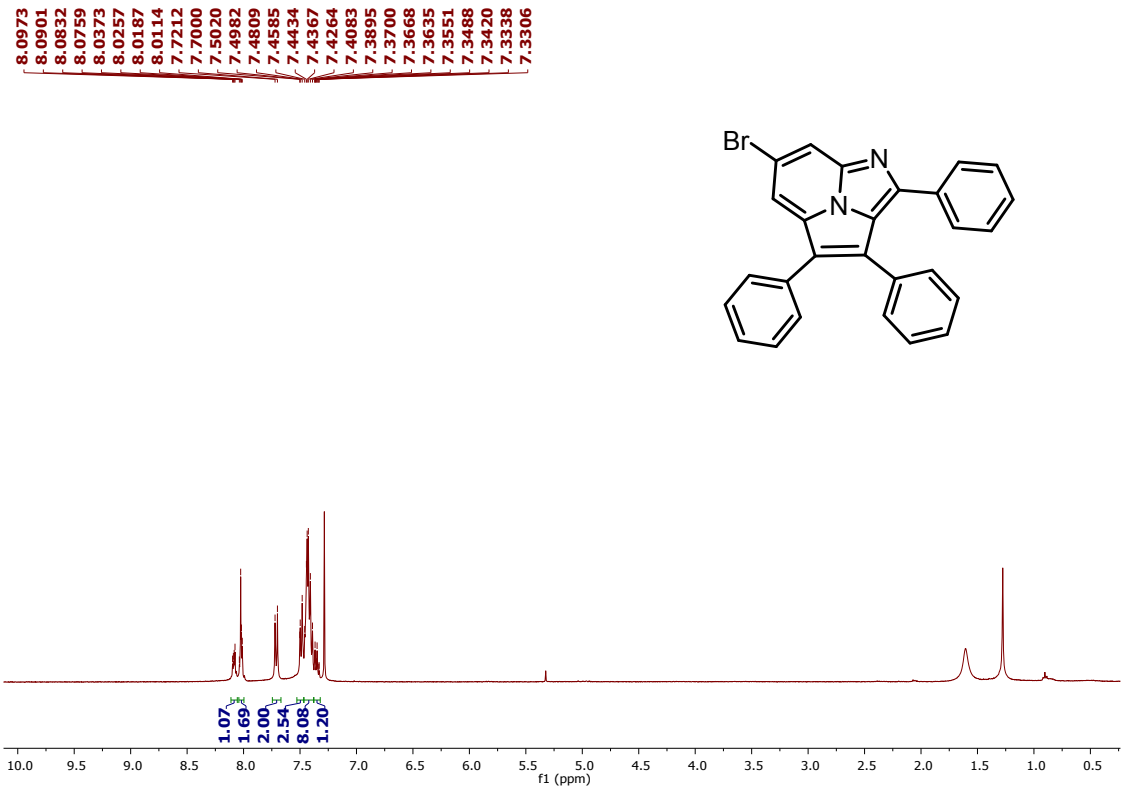

Figure s19. ^{1}H NMR spectrum of **6d**.

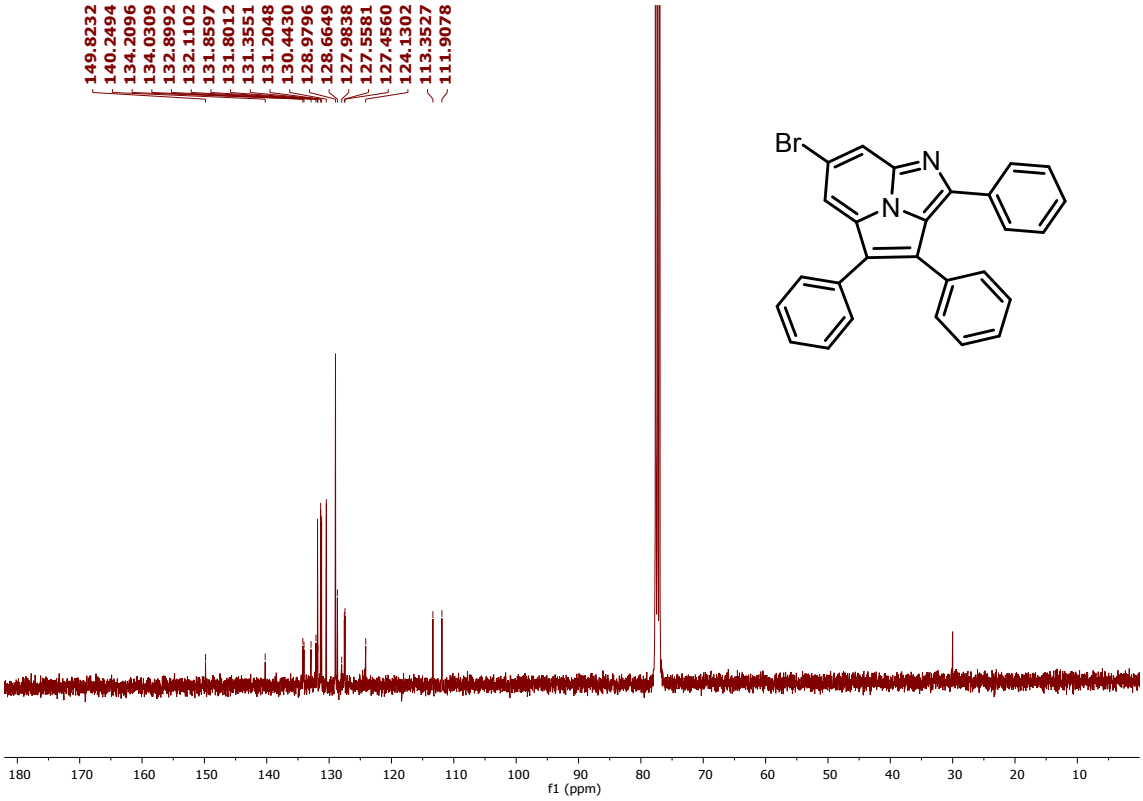

Figure s20. ^{13}C{^{1}H} NMR spectrum of **6d**.

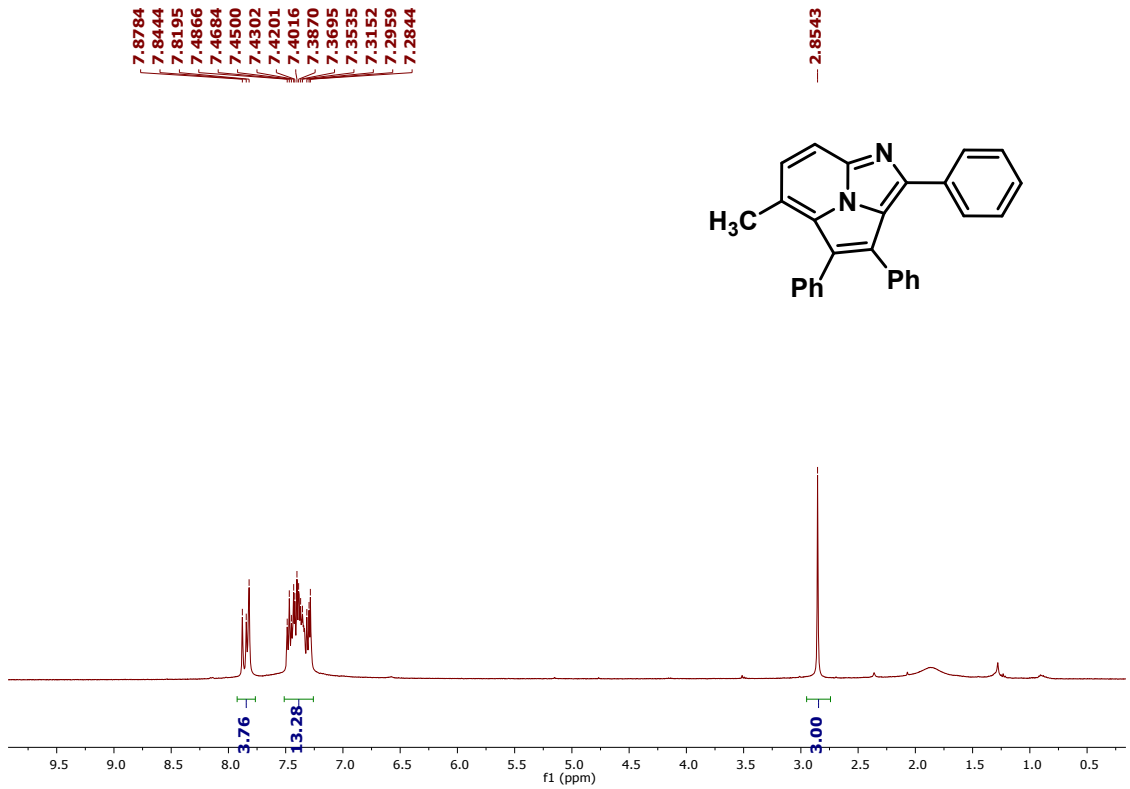

Figure s21. ^{1}H NMR spectrum of **6e**.

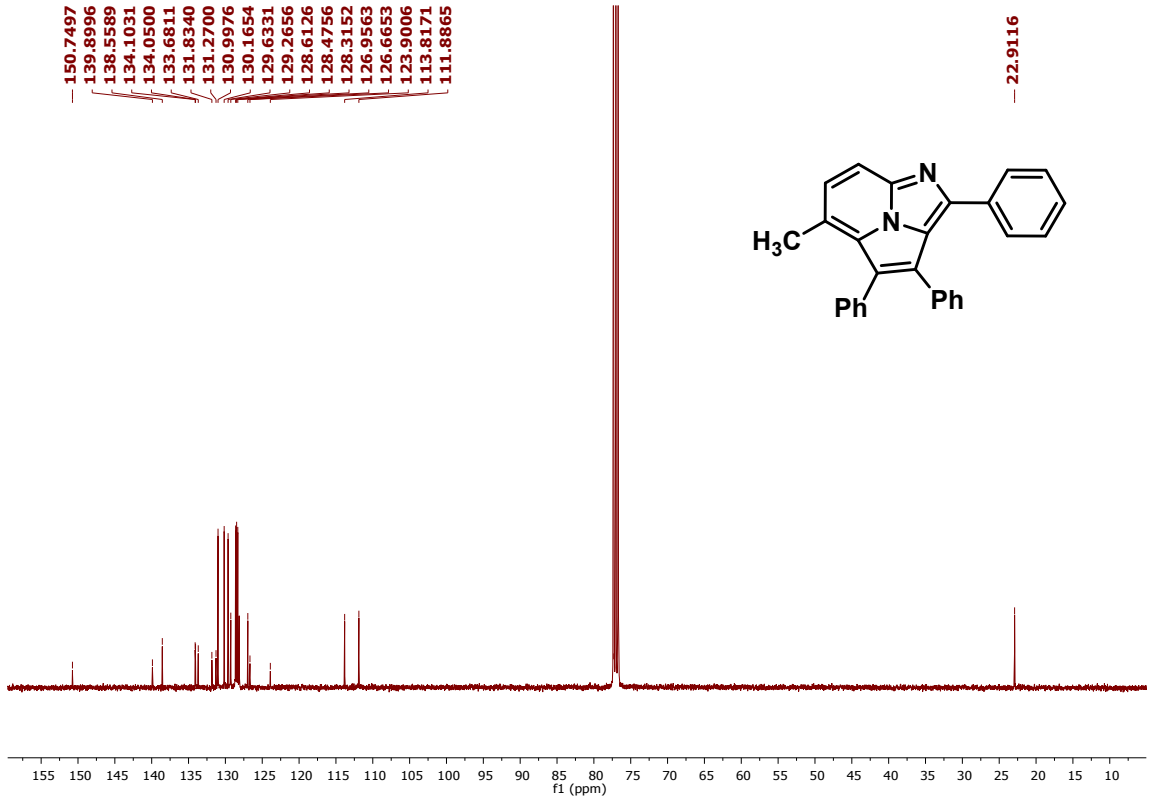

Figure s22. ^{13}C{^{1}H} NMR spectrum of **6e**.

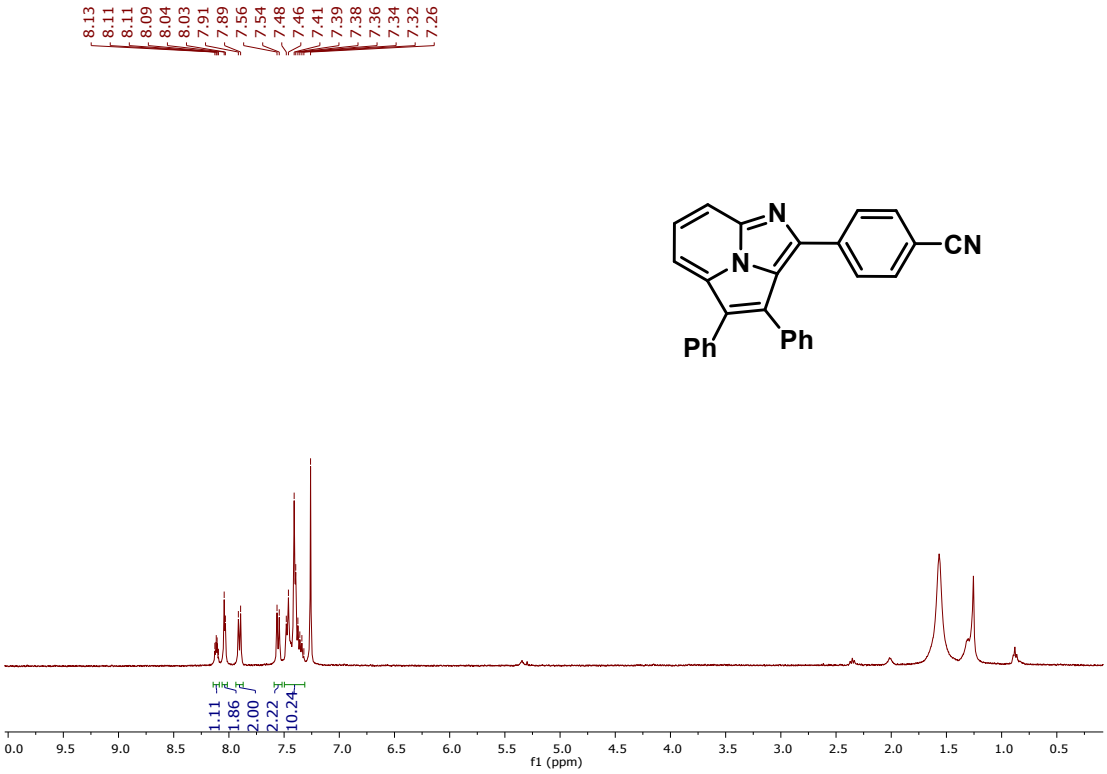

Figure s23. ^{1}H NMR spectrum of **6f**.

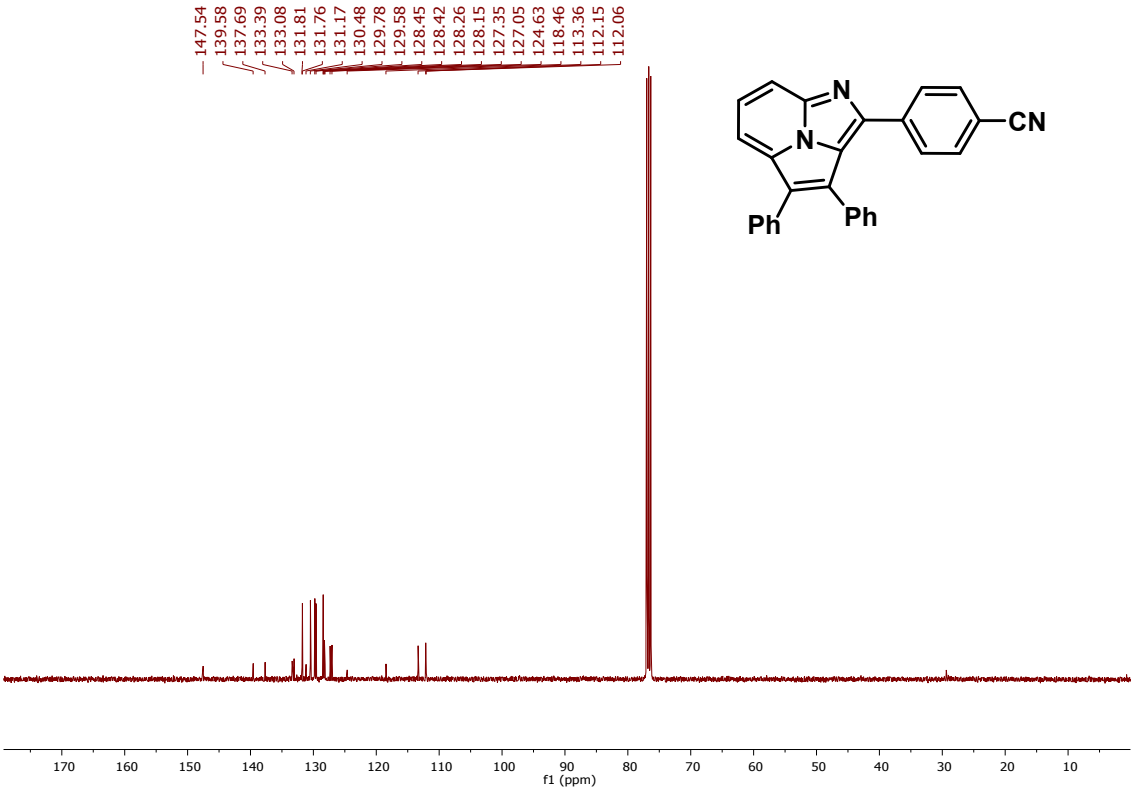

Figure s24. ^{13}C{^{1}H} NMR spectrum of **6f**.

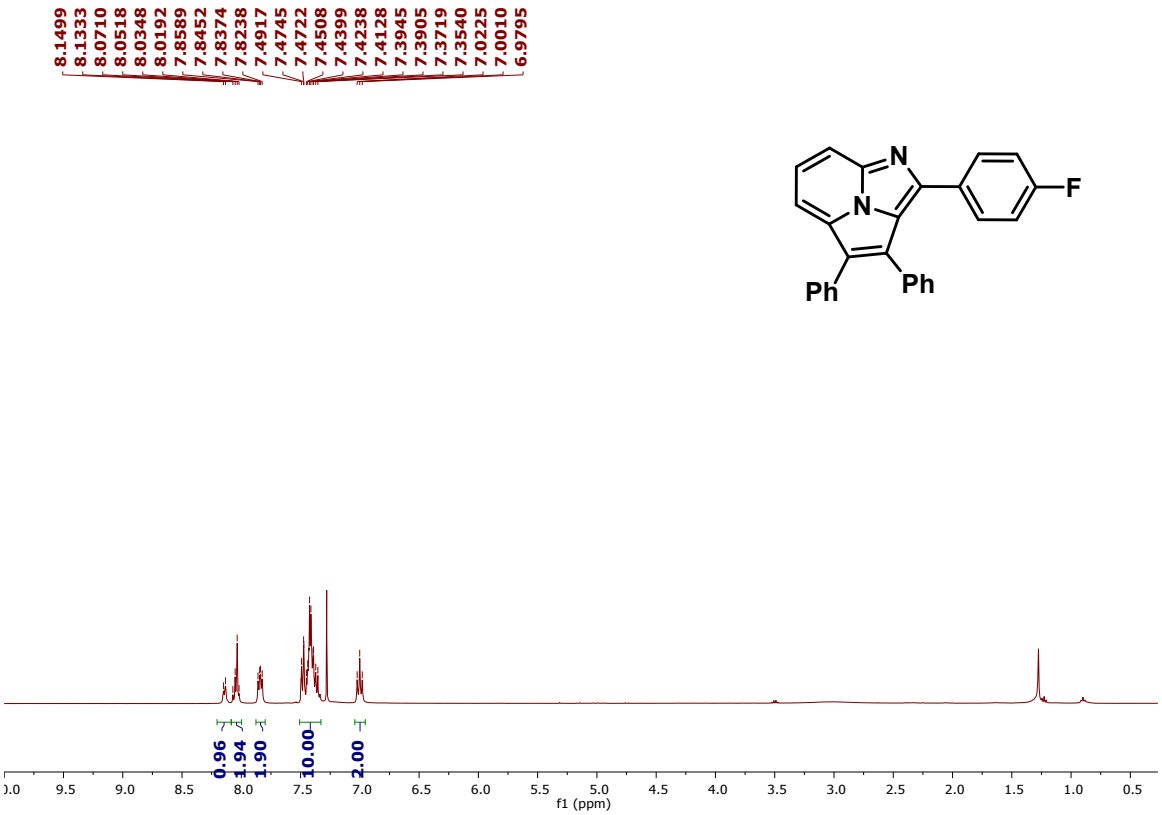

Figure s25. ^{1}H NMR spectrum of **6g**.

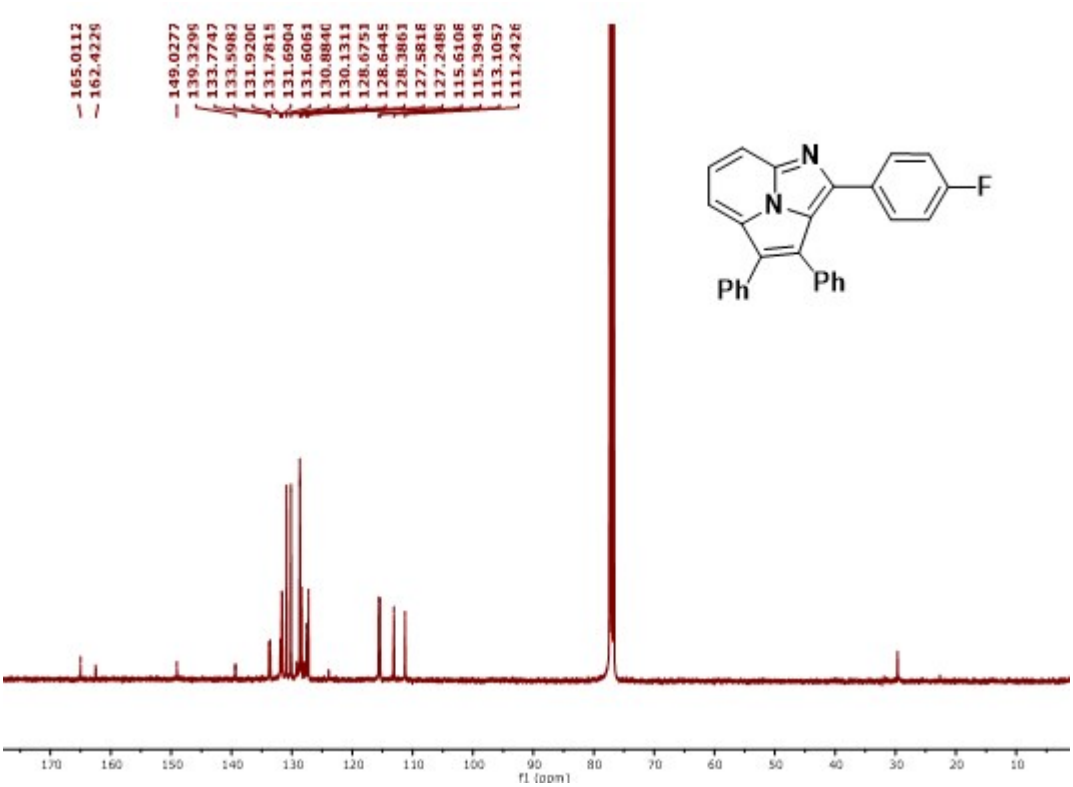

Figure s26. ^{13}C{^{1}H} NMR spectrum of **6g**.

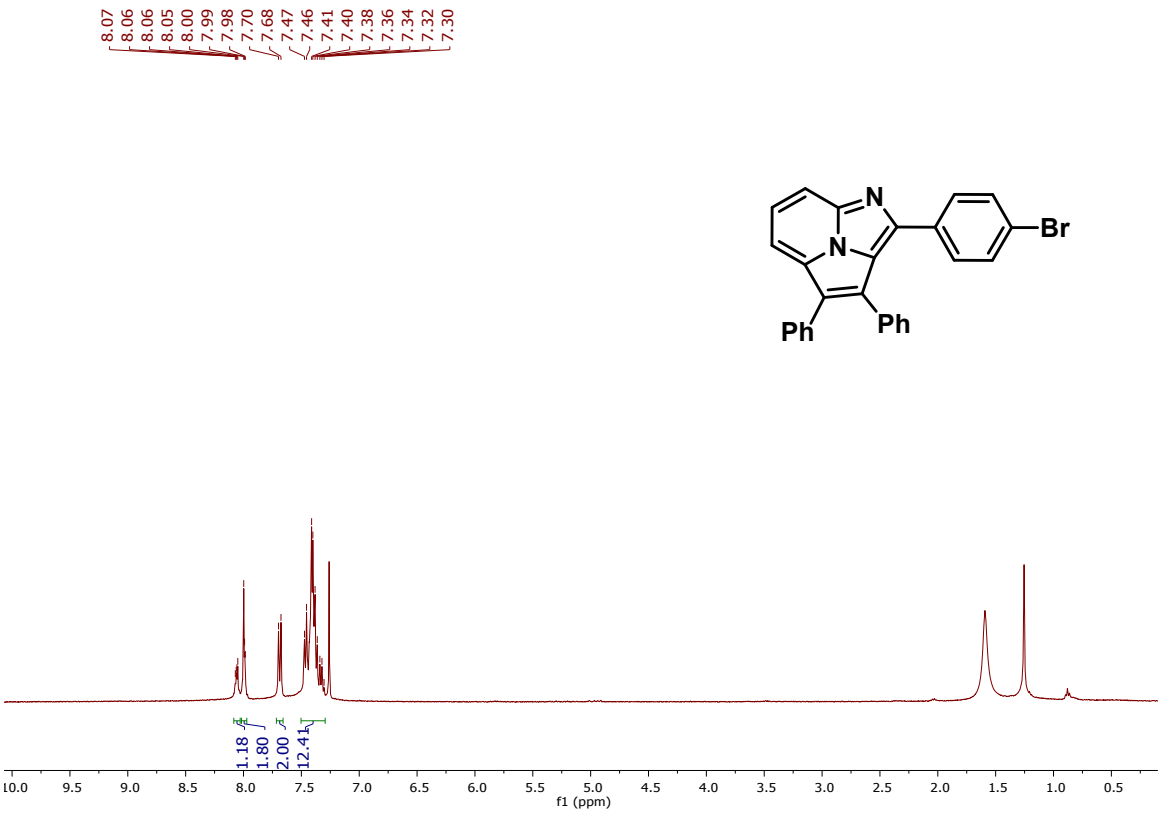

Figure s27. ^{1}H NMR spectrum of **6h**.

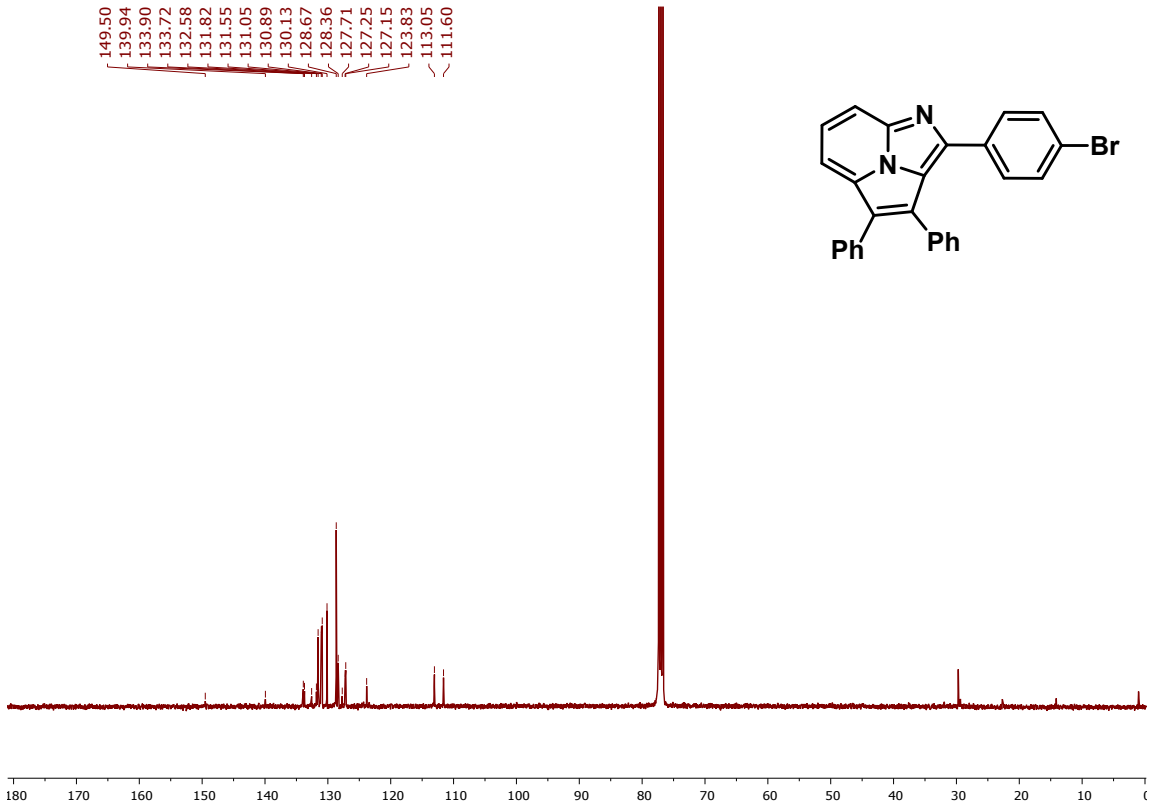

Figure s28. ^{13}C{^{1}H} NMR spectrum of **6h**.

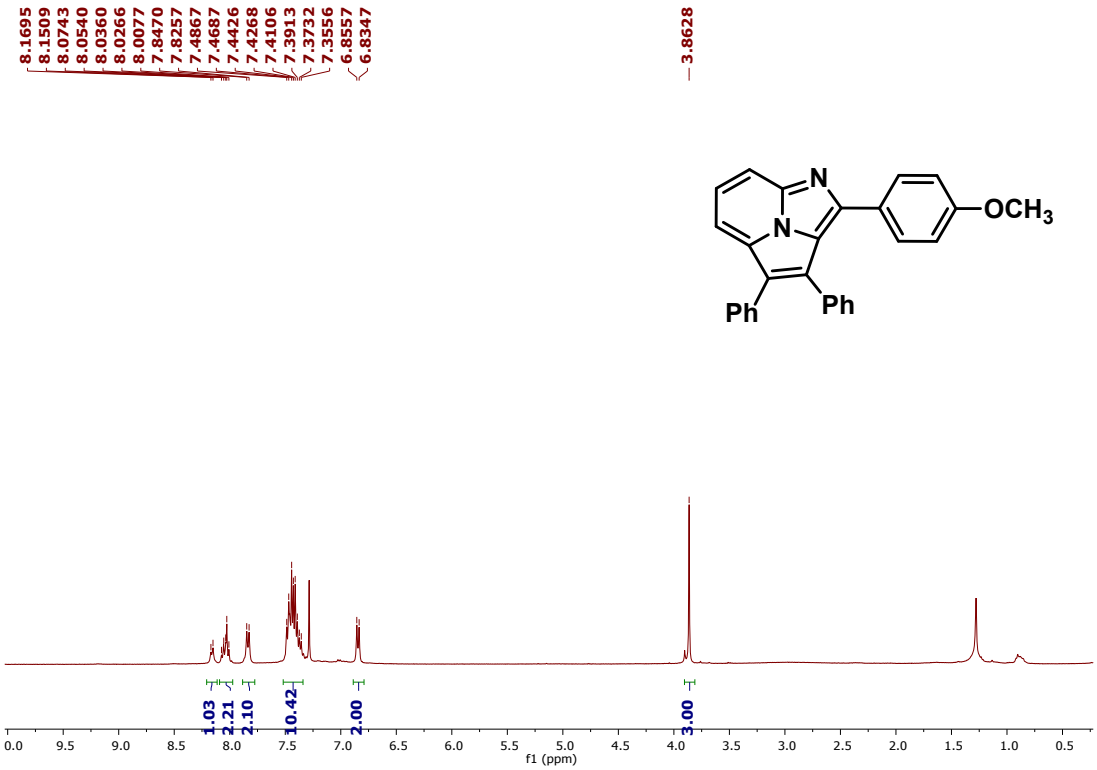

Figure s29. ^{1}H NMR spectrum of **6i**.

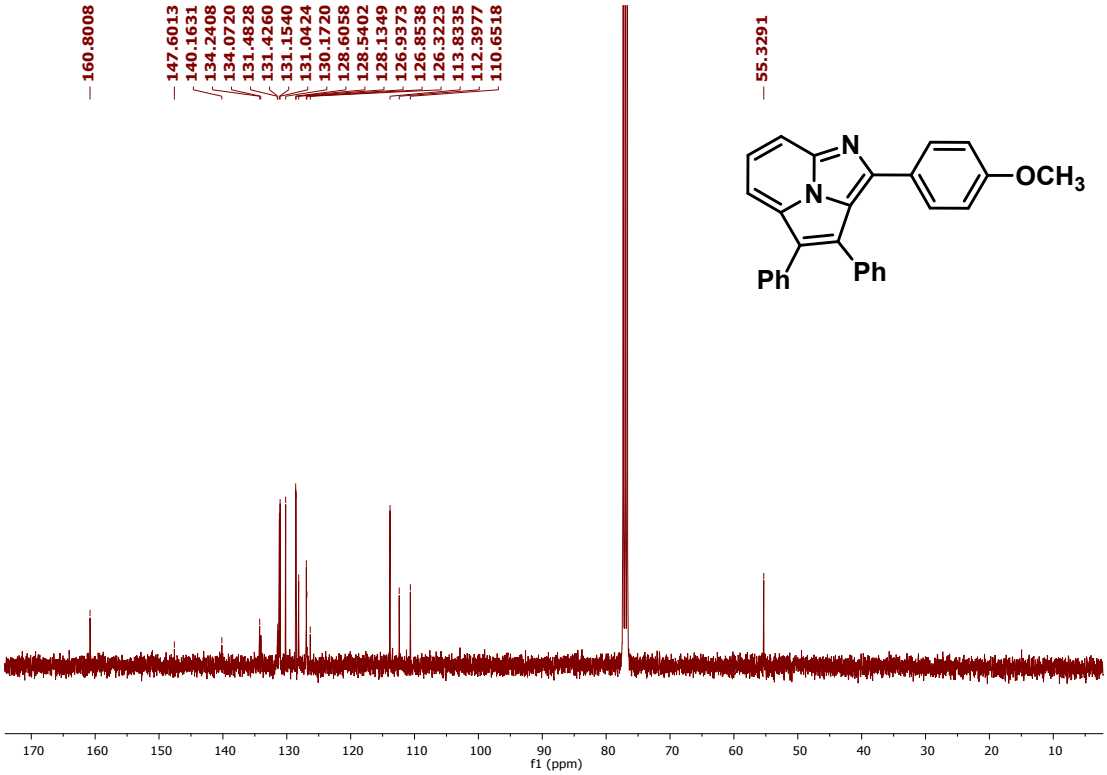

Figure s30. ^{13}C{^{1}H} NMR spectrum of **6i**.

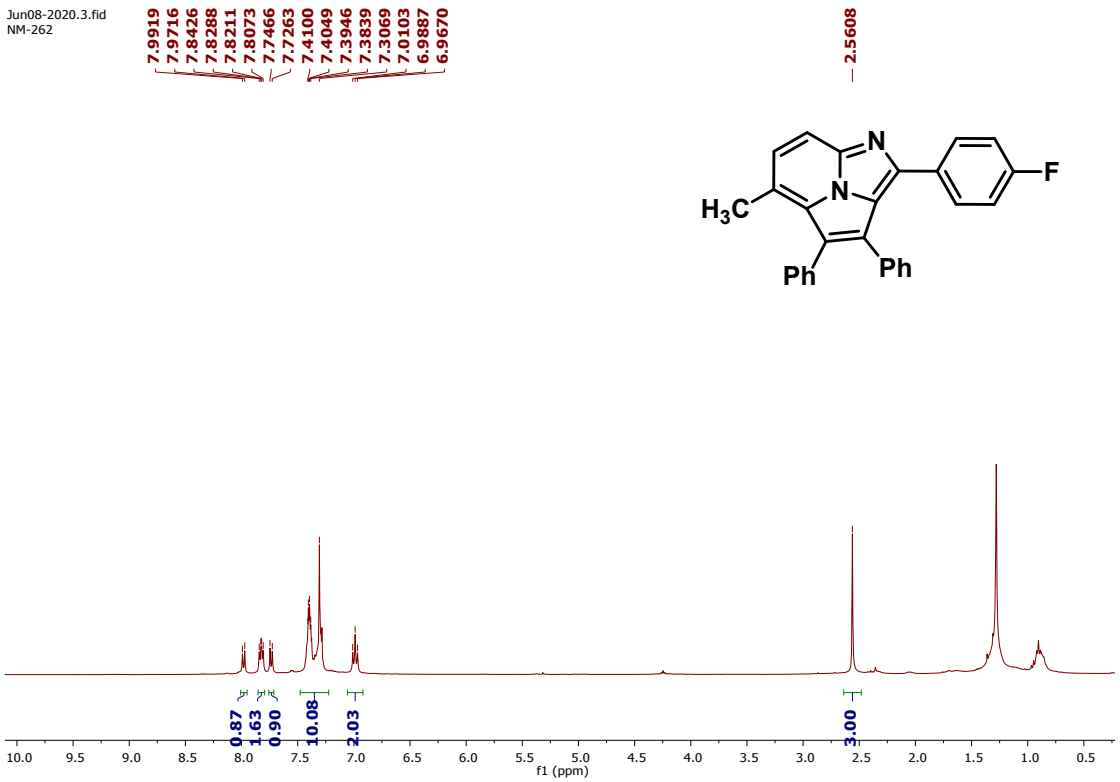

Figure s31. ^{1}H NMR spectrum of **6j**.

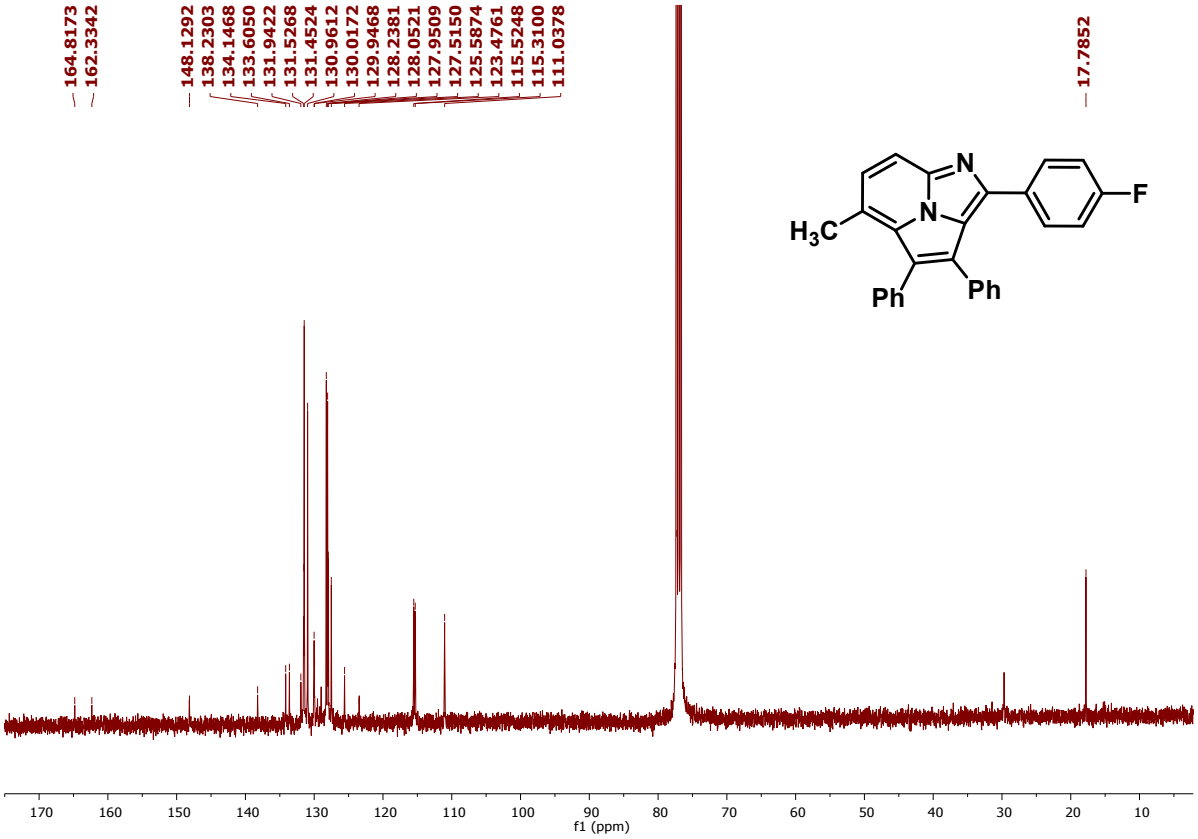

Figure s32. ^{13}C{^{1}H} NMR spectrum of **6j**.

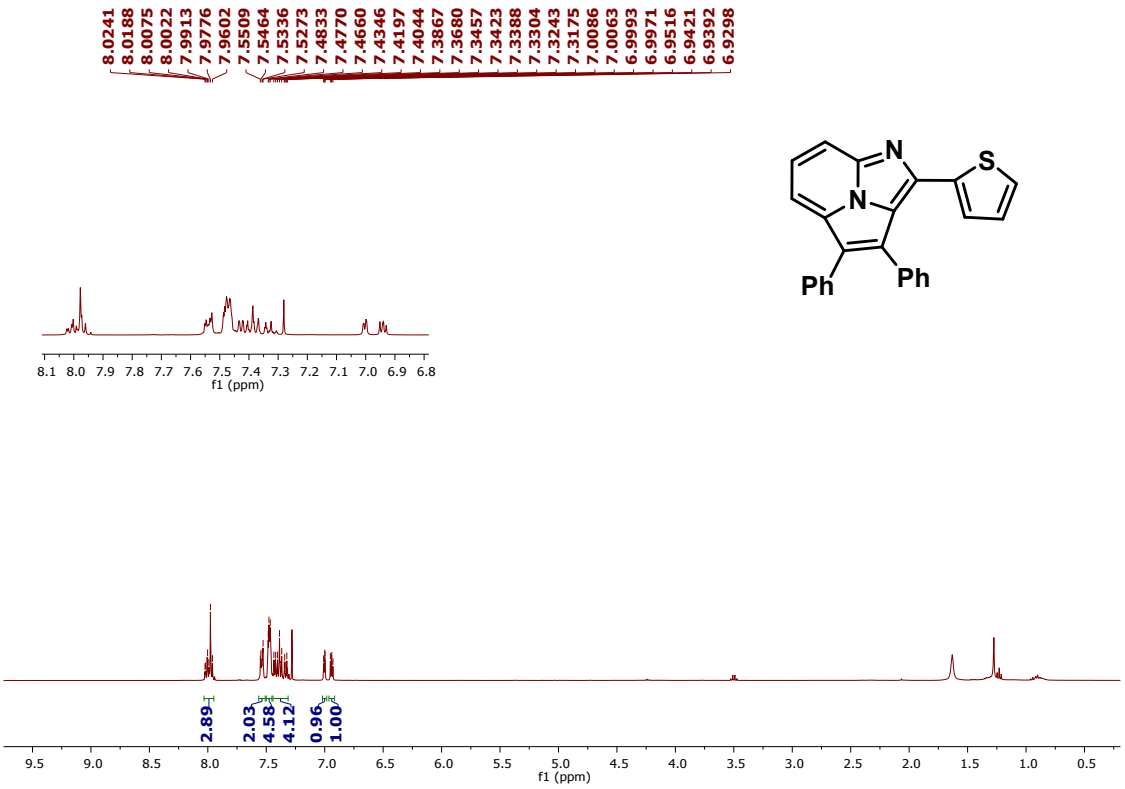

Figure s33. ^{1}H NMR spectrum of **6k**.

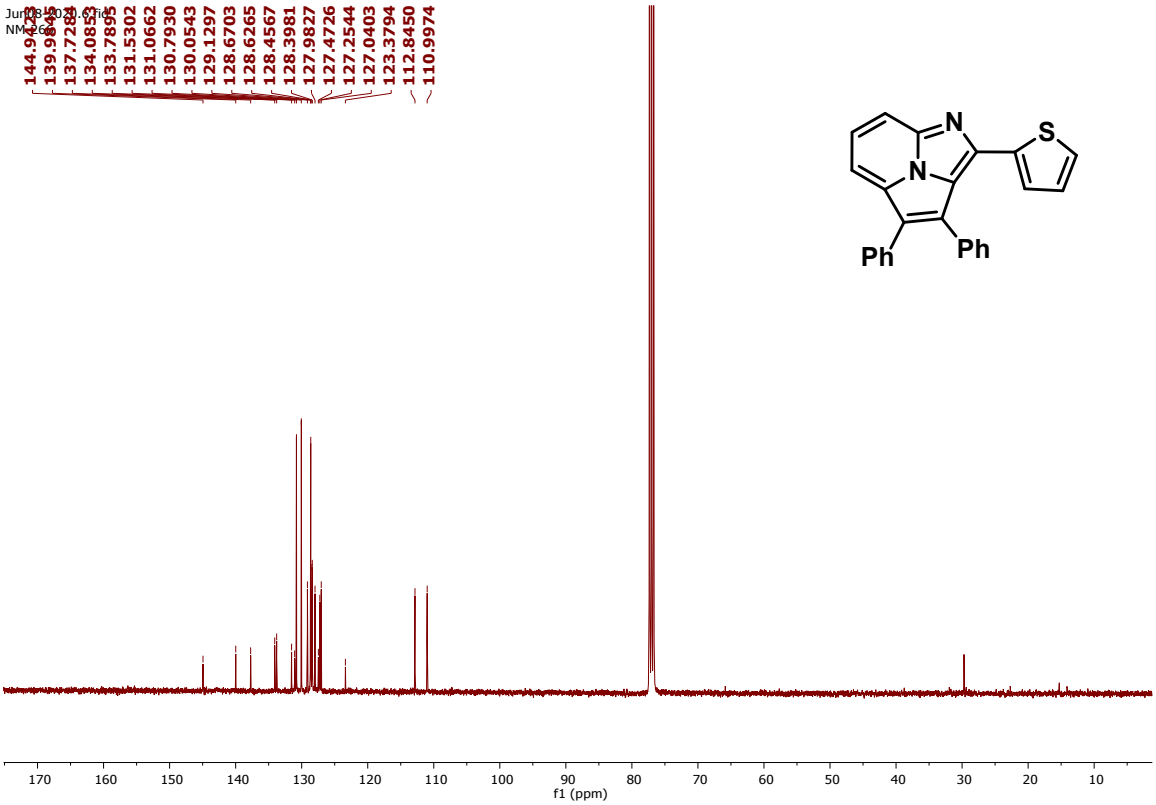

Figure s34. ^{13}C{^{1}H} NMR spectrum of **6k**.

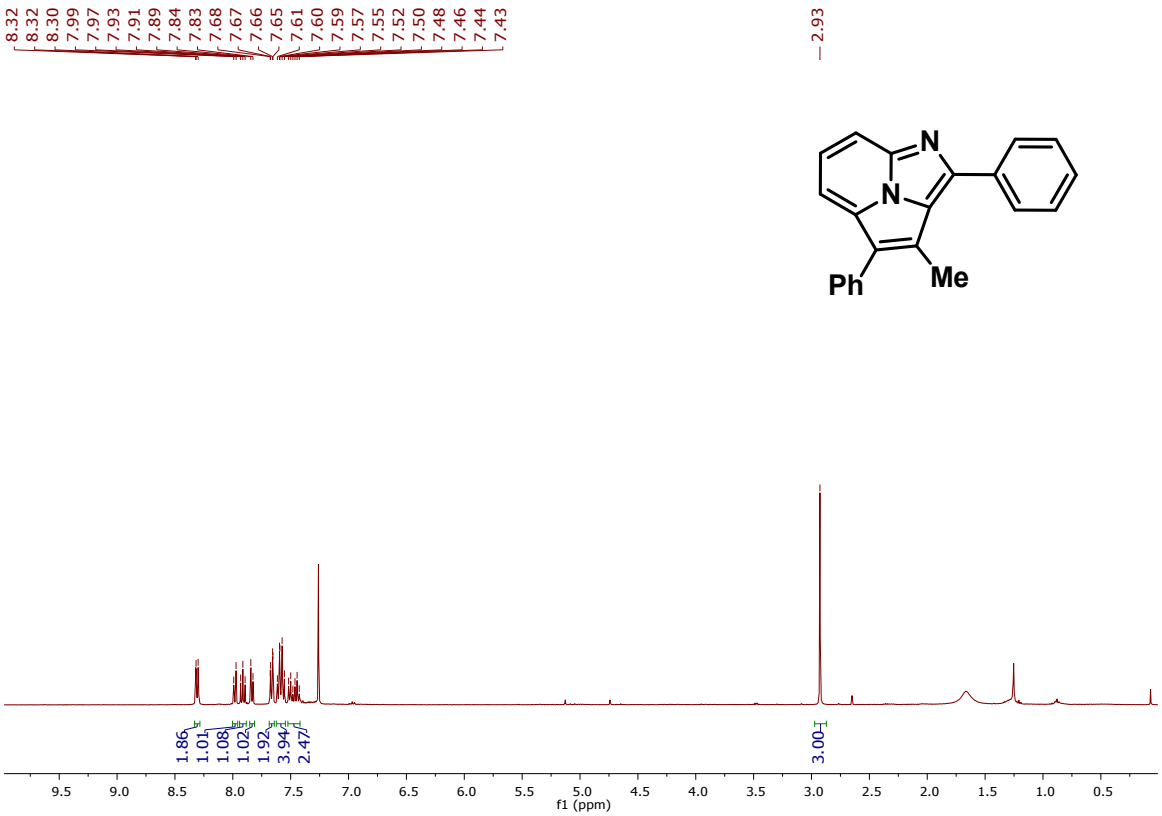

Figure s35. ^{1}H NMR spectrum of **6l**.

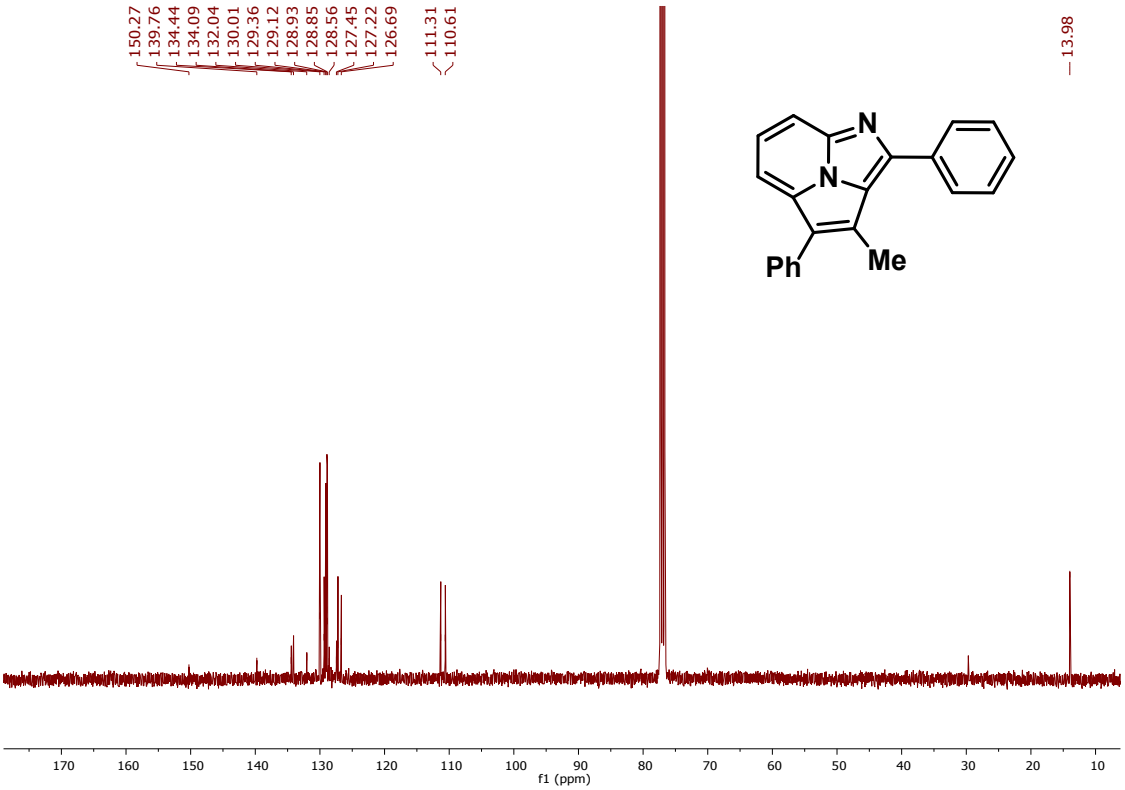

Figure s36. ^{13}C{^{1}H} NMR spectrum of **6l**.

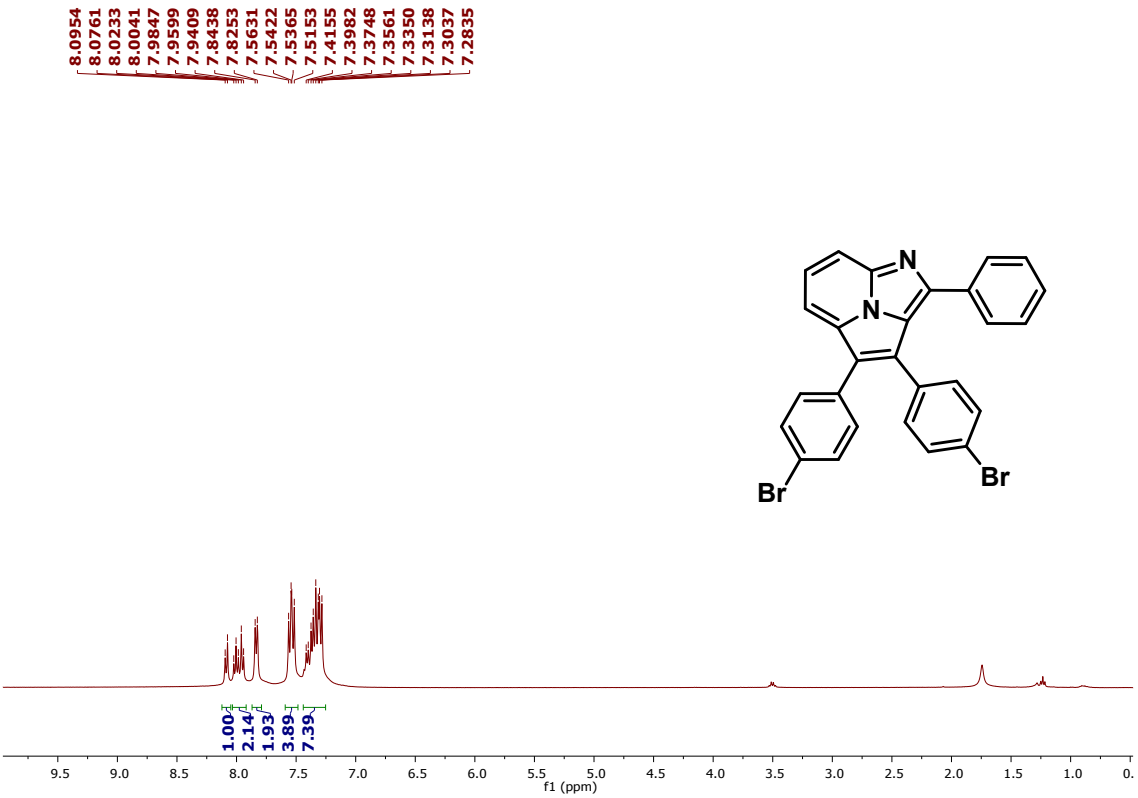

Figure s37. ^{1}H NMR spectrum of **6m**.

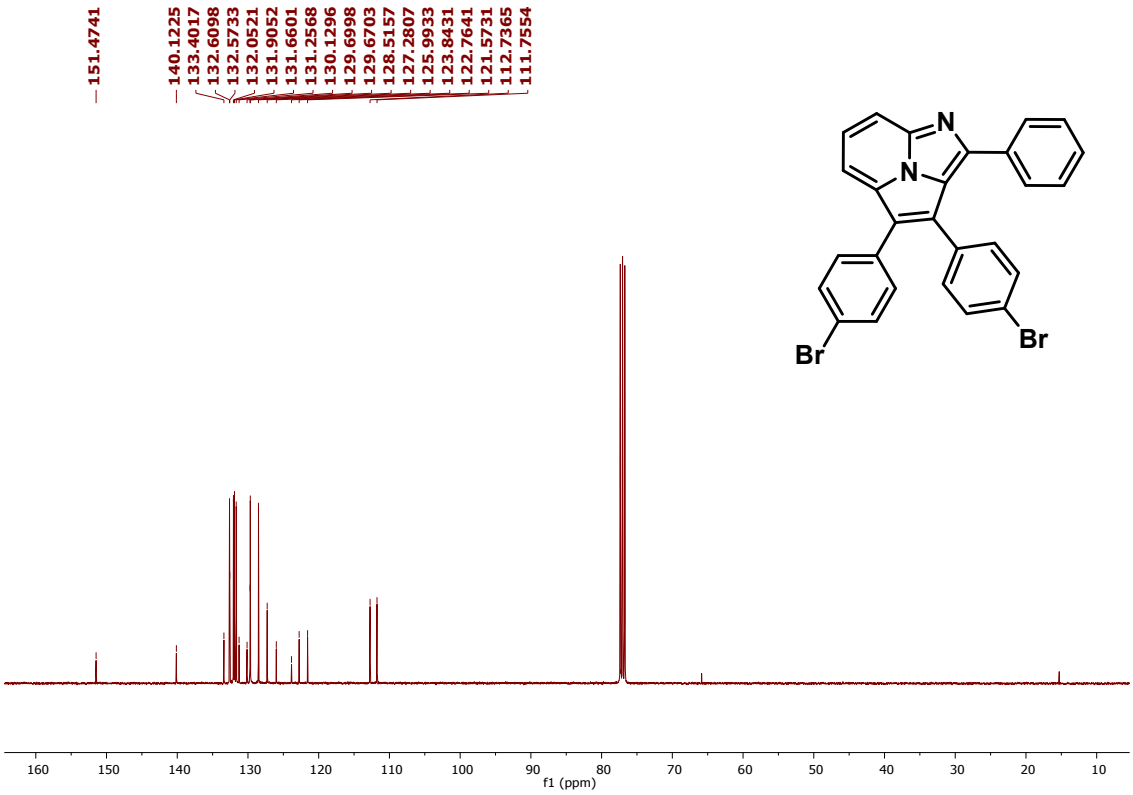

Figure s38. ^{13}C{^{1}H} NMR spectrum of **6m**.

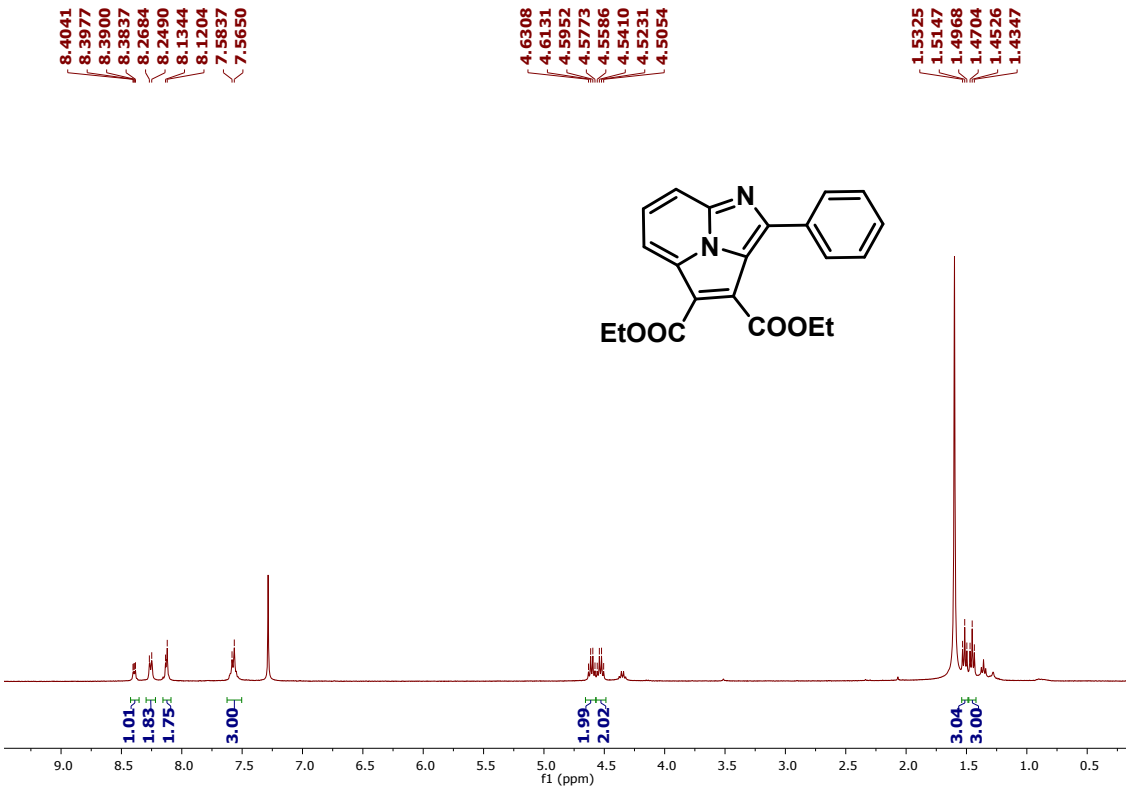

Figure s39. ^{1}H NMR spectrum of **6n**.

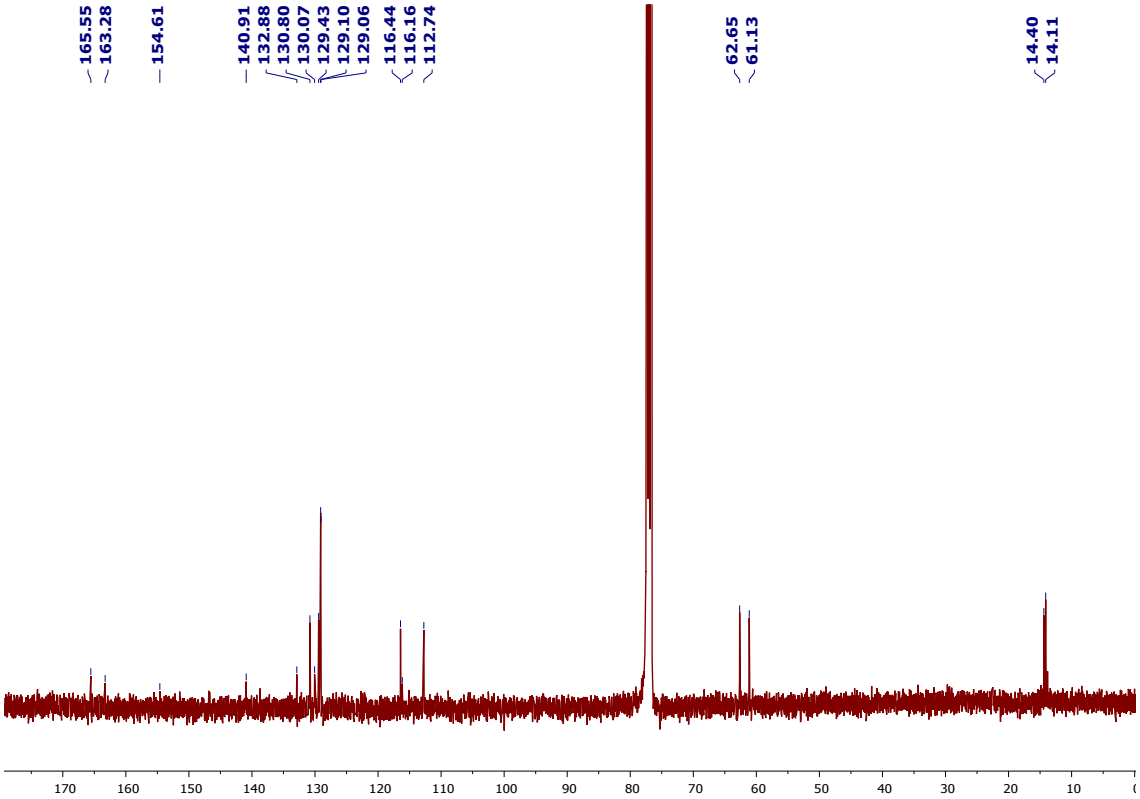

Figure s40. ^{13}C{^{1}H} NMR spectrum of **6n**.

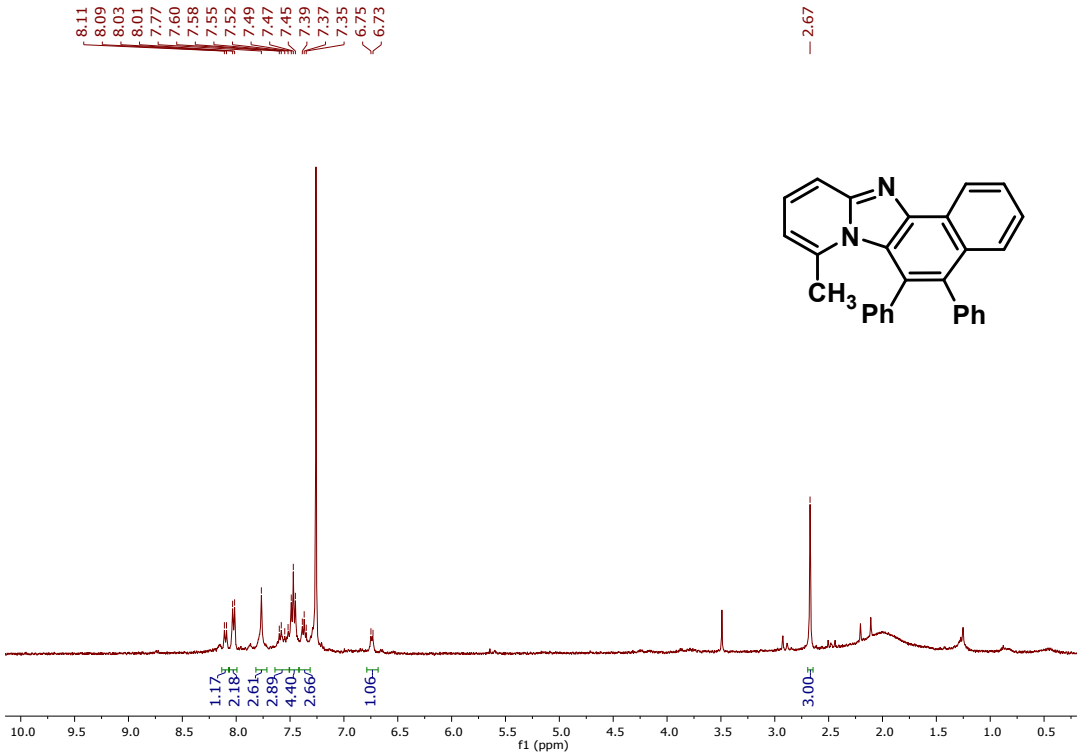

Figure s41. ^{1}H NMR spectrum of **70**.

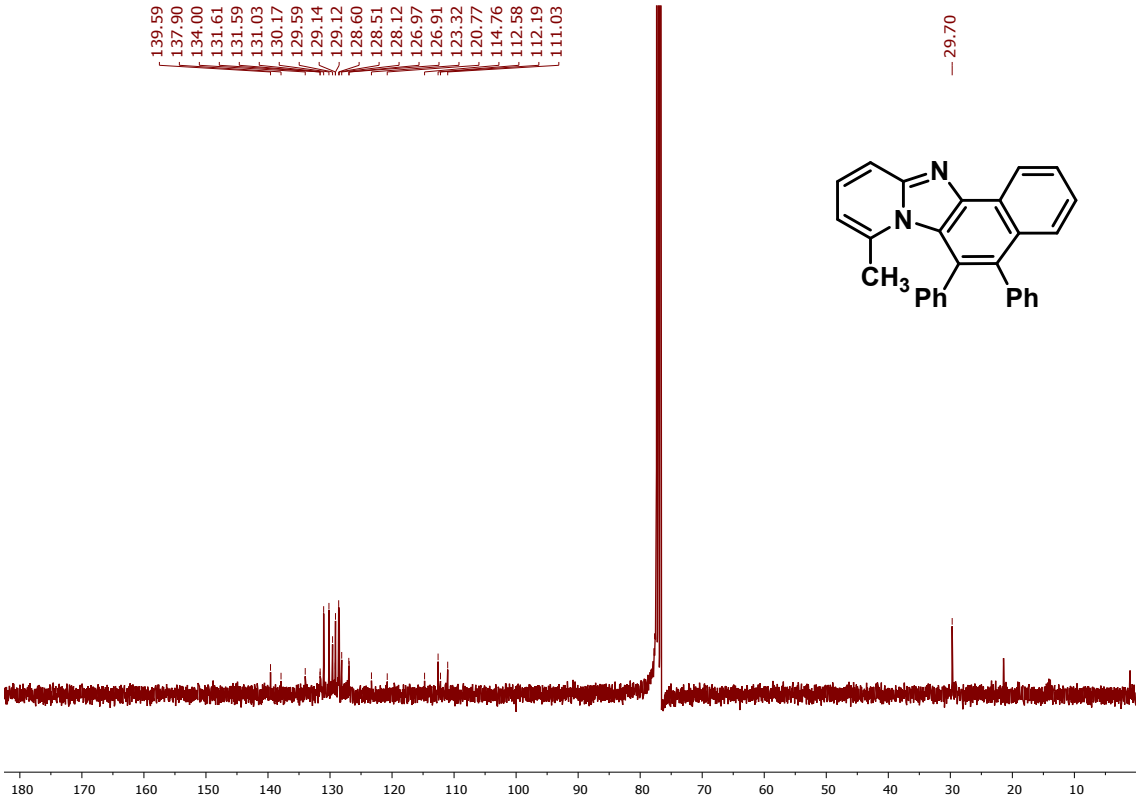

Figure s42. ^{13}C{^{1}H} NMR spectrum of **7o**.

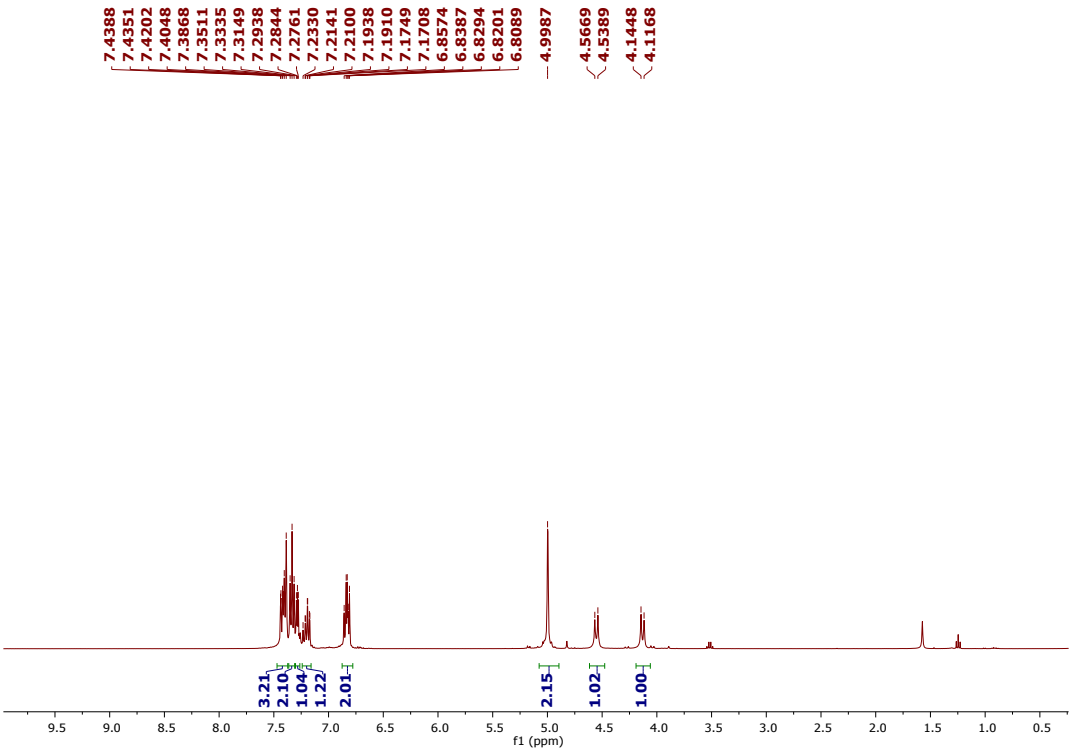

Figure s43. ^{1}H NMR spectrum of complex **3** after storing for three months at room temperature under open air conditions.

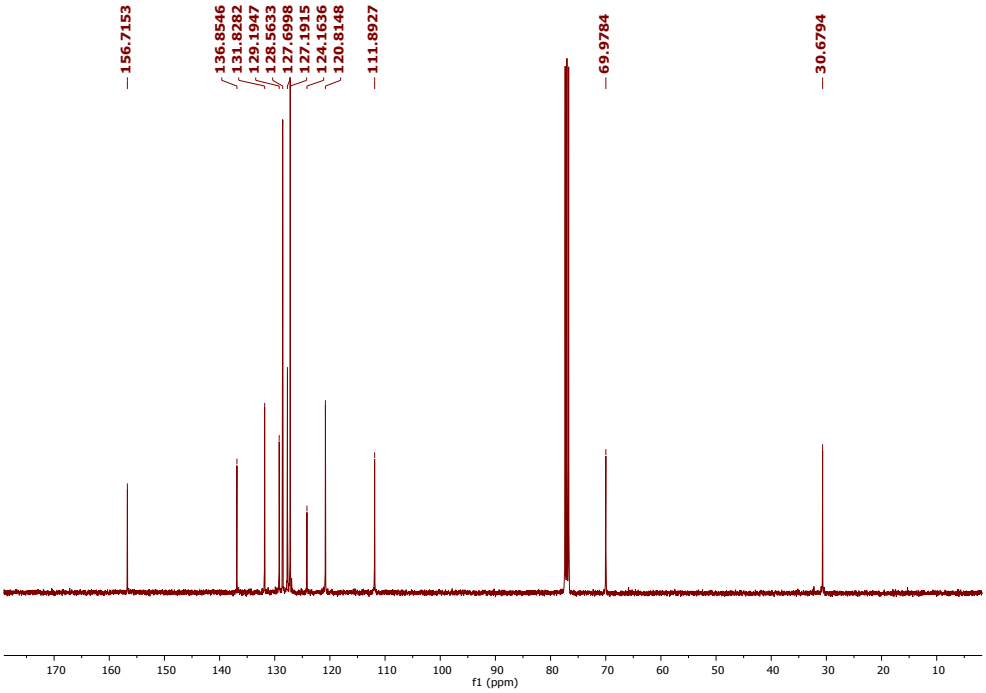

Figure s44. ^{13}C{^{1}H} NMR spectrum of complex **3** after storing for three months at room temperature under open air conditions.

(Note: Peaks at 0.86 and 1.26 ppm in HNMRs and 29.76 in CNMRs are due to grease whereas peak at 1.56 in HNMRs is due to moisture of $CDCl_3$)

REFERENCES

(s1) APEX3, Bruker AXS Inc., Madison, WI, USA, 2012.

(s2) G. M. Sheldrick, SADABS, Bruker AXS Inc., Madison, WI, USA, 2001.

(s3) (a) "A short history of SHELX", G. M. Sheldrick, *ActaCryst*. **2008**, *A64*, 112-122. (b) "SHELXT – Integrated space-group and crystal structure determination", G. M. Sheldrick, *ActaCryst*. **2015**, *A71*, 3-8. (c) "Crystal structure refinement with SHELXL", G. M. Sheldrick, *ActaCryst*. **2015**, *C71*, 3-8.

(s4) "OLEX2: A Complete Structure Solution, Refinement and Analysis Program", O. V. Dolomanov, L. J. Bourhis, R. J. Gildea, J. A. K. Howard, H. Puschmann, *J. Appl. Cryst*. **2009**, *42*, 339-341.

(s5) Single-crystal structure validation with the program "PLATON", A. L. Spek, *J. Appl. Cryst*. **2003**, *36*, 7-13.

(s6) J. VandeVondele, M. Krack, F. Mohamed, M. Parrinello, T. Chassaing, and J. Hutter, *Comput. Phys. Commun.*, **2005**, *167*, 103-128.

(s7) J. Hutter, M. Iannuzzi, F. Schiffmann, and J. VandeVondele, *Wiley Interdiscip. Rev.: Comput. Mol. Sci.*, **2014**, *4*, 15-25.

(s8) S. Goedecker, M. Teter, and J. Hutter, *Phys. Rev. B*, **1996**, *54*, 1703-1710.

(s9) J. VandeVondele and J. Hutter, *J. Chem. Phys.*, **2007**, *127*, 114105.

(s10) W. Humphrey, A. Dalke, and K. Schulten, *J. Mol. Graph.*, **1996**, *14*, 33-38.

(s11) (a) M. J. Plevin, D. L. Bryce, J. Boisbouvier, *Nat. Chem.* **2010**, *2*, 466-471. (b) S. Tsuzuki, K. Honda, T. Uchimaru, M. Mikami, K. Tanabe, *J. Am. Chem. Soc.* **2000**, *122*, 3746-3753. (c) S. Tsuzuki, K. Honda, T. Uchimaru, M. Mikami, K. Tanabe, *J. Am. Chem. Soc.* **2000**, *122*, 11450-11458. (d) S. Tsuzuki, K. Honda, T. Uchimaru, M. Mikami, A. Fujii, J. *Phys. Chem. A,* **2006**, *110*, 10163-10168. (e) S. Tsuzuki, *Annu. Rep. Prog. Chem., Sect. C Phys. Chem.*, **2012**, *108*, 69–95.

(s12) P. Li, X. Zhang, and X. Fan, *J. Org. Chem.* **2015**, *80*, 7508-7518.